

**STUDY OF INELASTIC RESPONSE OF OPEN-GROUND STOREY
RCC BUILDINGS**

A DISSERTATION

*Submitted in the partial fulfilment of the
requirements for the award of the degree
of*

MASTER OF TECHNOLOGY

in

EARTHQUAKE ENGINEERING
(With specialization in Structural Dynamics)

by

ZEESHAN ABBAS

(17526018)



**DEPARTMENT OF EARTHQUAKE ENGINEERING
INDIAN INSTITUTE OF TECHNOLOGY ROORKEE
ROORKEE-247 667 (INDIA)**

JUNE, 2019

CANDIDATE'S DECLARATION

I hereby, declare that the work which is being presented in this dissertation entitled, “**STUDY OF INELASTIC RESPONSE OF OPEN-GROUND STOREY RCC BUILDINGS**”, being submitted in partial fulfilment of the requirements for the award of degree of “Master of Technology” in “Earthquake Engineering” with specialization in Structural Dynamics, to the Department of Earthquake Engineering, Indian Institute of Technology Roorkee, under the supervision of **Dr. P. C. ASHWIN KUMAR**, Assistant Professor, Department of Earthquake Engineering, Indian Institute of Technology Roorkee, is an authentic record of my own work carried out during the period of June 2018 to June 2019.

I declare that I have not submitted the material embodied in this dissertation for the award of any other degree or diploma.

Place: Roorkee

Zeeshan Abbas

Date:

Enrollment no. 17526018

CERTIFICATE

This is to certify that the above statement made by the candidate is correct to the best of my knowledge and belief.

Place: Roorkee

Dr. P. C. Ashwin Kumar

Assistant Professor

Date:

Department of Earthquake Engineering
Indian Institute of Technology Roorkee

ABSTRACT

Reinforced Concrete (RC) frames with unreinforced masonry infills (URM) are the most commonly used construction practice in India and worldwide. The infills are generally treated as nonstructural elements and are not considered while designing because of the complexity attached to its interaction with the surrounding frame elements and lack of knowledge about its modelling. However, the presence of infills drastically increase the strength and stiffness thus affects the performance sufficiently. Increase in stiffness the infill frames attracts higher lateral forces for which the buildings are not designed generally. In addition to that the irregular placing of infills also adds to the vulnerability of the buildings.

In this study seismic performance of RC building with open ground storey has been studied. The considered building is 6 storey with an open ground storey located in a zone V of IS-1893 (2016) on a medium soil. The bare frame was first designed using Response spectrum analysis. Three cases are considered, where in each case the ground storey columns were designed for higher forces. After designing, Infills are modelled as Equivalent Strut elements and performance have been assessed under pushover and nonlinear time history analysis. For the first case the hinges pattern and the inter storey drift ratio has shown that the ground storey column and beams are most vulnerable. And over all the structure was vulnerable to soft storey mechanism. But in the later stages for Case 2 and Case 3 the performance improved in pushover analysis and also in case of nonlinear time history analysis.

ACKNOWLEDGEMENT

Foremost, I would like to express my gratitude to my supervisor **Dr. P. C. Ashwin Kumar**, Assistant Professor in Department of Earthquake Engineering, Indian Institute of Technology Roorkee, for the support and encouragement I received from him at all stages of my dissertation. Frequent discussions throughout the dissertation work were extremely fruitful and helped me to overcome hurdles and problems I faced during this work.

Further, I would like to acknowledge the extremely good computer facilities provided by the department without which this work would not have been possible.

Scholarship given by Ministry of Human Resources and Development, Government of India is highly appreciated for this dissertation work.

I am also thankful to my friend **Avanish Vatedka** for all the help and valuable discussions. I would like to thank **Ayushman Sharma** and **Zeeshan Manzoor Bhat** for their help and support.

My warmest thanks goes to all those who have helped me. My special thanks are due to **Sateesh Kumar Puri, Pradeep Mishra, Pavan Kumar, Aman Srivastava, Sajid Ali, Sahil Gulab Angural, and Iqbal Hussain.**

I would like to thank my parents **Nazir Hussain** and **Zenab Bibi** for their unconditional love.

Thanks to everyone who has helped me achieve this.

TABLE OF CONTENTS

CANDIDATE’S DECLARATION	ii
CERTIFICATE	ii
ABSTRACT.....	iii
ACKNOWLEDGEMENT	iv
TABLE OF CONTENTS.....	v
LIST OF FIGURES	vii
LIST OF TABLES.....	ix
CHAPTER 1: INTRODUCTION.....	1
1.1 General	1
1.2 Performance of Soft Storey RC Buildings in Earthquakes	1
1.3 Modes of failure in Masonry	2
1.3.1 Sliding Shear Failure	3
1.3.2 Corner Crushing Failure	3
1.3.3 Diagonal Tension Failure	3
1.3.4 Frame Failure.....	3
CHAPTER 2: MODELLING OF URM INFILLED RC FRAMES.....	4
2.1 General	4
2.2 IS Code provisions	4
2.3 Modelling of RC members	5
2.4 Modelling of URM Infills	6
2.4.1 Macro Modeling of URM Infills	7
2.5 Hysteretic Modelling.....	9
CHAPTER 3: MODELLING AND ANALYSIS OF BUILDING	11
3.1 Building Description	11
3.2 Modelling	12
3.2.1 Inelastic Modelling.....	12
3.3 Determination of Design Lateral Force.....	13
3.3.1 Equivalent Static Method	14
3.3.2 Response Spectrum Method.....	15
3.4 Pushover Analysis	16
CHAPTER 4: NONLINEAR DYNAMIC ANALYSIS.....	17
4.1 Ground Motion Selection	17

4.2	Amplitude Scaling	17
4.3	Damping	19
4.4	Hysteretic Model	20
CHAPTER 5: RESULTS AND CONCLUSIONS		21
5.1	Modal Analysis.....	22
5.2	Base Shear	23
5.3	Stiffness Variation due to the Infills.....	24
5.4	Design Forces	25
5.5	Storey Displacement and Inter Storey Drift Ratio	25
5.6	Pushover Analysis	27
5.7	Time History Analysis.....	29
5.7.1	Base Shear	29
5.7.2	Storey Displacement and Inter Storey Drift Ratio.....	31
5.8	Design Cases	35
5.8.1	Base Shear	36
5.8.2	Pushover Analysis	36
	Inter Storey Drift Ratio	40
CHAPTER 6: CONCLUSIONS		42
REFERENCES		43

LIST OF FIGURES

Figure 1.1 Failure of buildings with Soft Storey during Bhuj Earthquake, (2001).(IITK.ac.in)	2
Figure 2.1 Generalised force-deformation behaviour of a typical RC member to define performance limit state under flexure as per ASCE-41 (2016)	6
Figure 2.2 Idealized stress strain relationship for masonry (Kaushik <i>et al</i> , 2007)	9
Figure 3.1 Plan of the considered building	11
Figure 3.2 Validation of the sap auto hinge with IS-456 (2000)	13
Figure 3.3 IS-1893 Part-1 (2016) spectra for Response Spectra Method	15
Figure 4.1 Selected ground motions	19
Figure 4.2 Rayleigh damping	19
Figure 4.3 Isotropic Hysteresis modal (SAP 2000)	20
Figure 5.1 First three mode shapes for the Bare frame in transverse direction	23
Figure 5.2 First three mode shapes for the Infilled frame in transverse direction	23
Figure 5.3 Comparison of roof displacement for bare and infilled frame under static condition in transverse direction	26
Figure 5.4 Comparison of roof displacement for bare and infilled frame under static condition in longitudinal direction	26
Figure 5.5 Inter Storey Drift ratio in transverse direction in case of linear static method	27
Figure 5.6 Inter Storey Drift ratio in longitudinal direction in case of linear static method	27
Figure 5.7 Comparison of pushover curve in (a) longitudinal and (b) transverse direction for Case 1	28
Figure 5.8 Hinge formation pattern in pushover transverse direction	28
Figure 5.9 Hinge formation pattern in pushover analysis longitudinal direction	29
Figure 5.10 Comparison of roof displacement in transverse direction with and without Infills in NLTH analysis	31
Figure 5.11 Comparison of roof displacement in longitudinal direction with and without Infills in NLTH analysis	31
Figure 5.12 Inter-storey drift ratio for the Case 1 bare frame in transverse direction ...	32
Figure 5.13 Inter-storey drift ratio for Case 1 infilled in transverse direction	32

Figure 5.14 Inter-storey drift ratio for the Case 1 bare frame along longitudinal direction	33
Figure 5.15 Inter-storey drift ratio for the Case 1 Infilled frame along longitudinal direction	33
Figure 5.16 Hinge formation pattern for Case 1 infilled frame	34
Figure 5.17 Hinge formation pattern for Case 1 infilled frame	34
Figure 5.18 Comparison of capacity curve for all the three cases along transverse direction	36
Figure 5.19 Hinge formation pattern for Case 3 in pushover analysis along the longitudinal direction	37
Figure 5.20 Hinge formation pattern for Case 3 in pushover analysis along the transverse direction	37
Figure 5.21 Comparison of IDR for three cases in Nonlinear Time History analysis along the transverse direction	40
Figure 5.22 Comparison of IDR for three cases in Nonlinear Time History analysis along longitudinal direction	40
Figure 5.23 Hinge formation pattern for Case 3 in longitudinal direction in NLTH analysis	41
Figure 5.24 Hinge formation pattern for Case 3 in transverse direction condition in NLTH analysis	41

LIST OF TABLES

Table 2.1 Effective stiffness of RC members as per IS-1893(2016)	6
Table 3.1: Sizes of Beams and Columns.....	12
Table 4.1 Details of ground motion records selected for NLTH analysis	18
Table 5.1 Modelling and design parameters	21
Table 5.2 Effect of Infills on the Period of Vibration	22
Table 5.3 Modal mass participation in fundamental mode of vibration	22
Table 5.4 Base Shear and Correction factor bare frame	24
Table 5.5 Base Shear comparison between bare and infilled frame.	24
Table 5.6 Variation of stiffness due to Infills	25
Table 5.7 Design forces in ground storey columns in transverse direction.	25
Table 5.8 Design forces for ground storey columns in longitudinal direction.....	25
Table 5.9 Base Shear for transverse frame with and without Infills in case of Nonlinear Time History analysis	30
Table 5.10 Base Shear for longitudinal frame with and without Infills in case of Nonlinear Time History analysis	30
Table 5.11 Column sizes and rebar % for different cases of design along transverse direction	35
Table 5.12 Column sizes and rebar % for different cases of design along longitudinal direction	35
Table 5.13 Base shear for all the three cases in linear static case.....	36
Table 5.14 Nonlinear Time History Base shear for different cases in transverse direction	38
Table 5.15 Nonlinear Time History Base shear for different cases in longitudinal direction	39

CHAPTER 1: INTRODUCTION

1.1 General

Reinforced Concrete frames with unreinforced masonry (URM) Infills are mostly used construction practice in many countries because of its availability and durability solutions. Masonry infill walls have very high compressive strength and initial stiffness so although its presence may increase the structural resistance but it may affect the capacity of the structure and also increase the seismic demand. Such buildings after the failure in masonry, creates a way for more severe damage to the building due to the sudden change in stiffness. Masonry walls are considered non-structural element and are mostly used as partition walls, and thus mainly on the basis of architectural and functional demand it may arise an irregularity in terms of stiffness strength and mass. The unsymmetrical arrangements of walls create an eccentricity between the center of mass and center of stiffness thus inducing a torsion in the structure under lateral load (Pauley and Priestly, 2009).

One of the major sources of such irregularity are absence of Infills in some storeys. In India it is a common practice of keeping ground storeys of multi-storey buildings open for parking or some other commercial purpose. The combination of in-plane stiffness of infill and flexural stiffness of RC frame induces a significantly high stiffness in the upper storeys than in lower (Haldar *et al*, 2013). This increases the possibility of soft storey mechanism .i.e. hinges will form in ground storey columns, and failure in columns are often governed by brittle shear, if they are not provided by sufficient transverse reinforcement.

1.2 Performance of Soft Storey RC Buildings in Earthquakes

In soft storey buildings the upper storeys with masonry Infills will almost act as one stiff component thus, the displacements at the roof level is nearly equal to the displacement at the soft storey. Hence the open ground storey will have a seismic response quite similar to a (SDOF) system, where the ground storey columns will represent the spring stiffness and the weight of the building will be the mass of the system. So the ground storey columns are subjected to a very high shear and flexure demand which the current practice does not accounts for, hence these type of structures

very much vulnerable to severe damage or even to complete collapse in case of an earthquake event.

From the surveys from the past earthquake events have shown that the open ground storeys faced high damage in ground storey columns and very negligible damage in the upper storeys. In Bhuj Earthquake around 1500 multi storey buildings collapsed by soft storey mechanism (Jain *et al.*, 2001).Figure 1.1 shows the failure of buildings in 2001 Bhuj Earthquake. Only the ground storey columns failed while the upper part of the structure remaining almost un damaged. Thus, the ground storey columns play a vital role in governing the performance of such irregular structures.



Figure 1.1 Failure of buildings with Soft Storey during Bhuj Earthquake, (2001).(IITK.ac.in)

1.3 Modes of failure in Masonry

Failure mechanism of an infilled frame mostly depends on relative stiffness and strength of infill and the frame. Other factors like the interface between the frame and infill wall, gap and openings in the Infills also governs the type of failure.

1.3.1 Sliding Shear Failure

Sliding shear failure occurs when brick elements have relatively higher strength than the mortar used or shear stress in the panel is higher than the compressive stress normal to brick mortar layers, there will be stepped type failure. Such failure are observed at the bed joint of the walls (Kaushik *et al*, 2006b)

1.3.2 Corner Crushing Failure

This type of failure is associated with system of very weak infill which is surrounded by strong frame.

1.3.3 Diagonal Tension Failure

Diagonal failure occurs when the principle tensile stress in the bricks exceeds the resistance, thus forming diagonal cracks. Diagonal tension cracks are generally develops in the direction opposite to the diagonal compression under in-plane loading.

1.3.4 Frame Failure

This failure generally occurs in the form of plastic hinge in frame members and connections.

CHAPTER 2: MODELLING OF URM INFILLED RC FRAMES

2.1 General

In general structures are designed in such a way that it remains in elastic range. However, in case of an earthquake loading the structure is expected to undergo displacement in inelastic range and also there will be a significant amount of dissipation of energy, thus the structure is designed for lower forces than elastic forces. Since there is very less insight in the expected performance and possible failure in seismic design codes it is a necessity to perform a nonlinear analysis. To understand and to be able to get an insight in the expected seismic performance and the possible damage pattern, understanding about the role played by stiffness, ductility and strength is important. This demands for a realistic simulation of the inelastic behavior of structures thus a proper model has to be developed which will cover up all the aspects that contributes to the overall behavior of structures. There are various ways to describe the nonlinear behavior of the structural element; in this paper, lumped plasticity model has been used as it simplifies the computational complexity without compromising with the accuracy.

The performance of a framed building is definitely affected by the presence of URM infills. To understand the behavior of URM infilled frames under seismic loading it is a complex procedure, thus a simpler analytical model is used i.e. macro modelling by way of equivalent struts as proposed by different researchers.

To estimate the response of the structure in dynamic nonlinear loading, the mechanism by which the energy is dissipated is studied which is incorporated by using hysteretic models. This chapter deals with modelling of reinforced framed buildings with and without URM and tries to provide design philosophy for open ground storey buildings.

2.2 IS Code provisions

Indian standard code for seismic design IS-1893 (2016) has defined two levels of seismic hazard i.e. Maximum Considered Earthquake (MCE) and Design Basis Earthquake (DBE). As per IS 1893 (2016) the base shear can be calculated as

$$V_B = \left(\frac{Z}{2} \frac{I}{R} \frac{S_a}{g} \right) W \quad (1.1)$$

Where, Z is zone factor it represents the Effective Peak Ground Acceleration (EPGA) for MCE and in case of DBE, it is considered half of EPGA in MCE. I is the importance factor, R being Response Reduction Factor. S_a is the spectral acceleration obtained from the response spectrum of code that is dependent on the natural time period of the building.

As per IS-1893 (2016) the design natural period of RC frame buildings with and without URM Infills can be computed by the following empirical formula

$$T = \frac{0.09H}{\sqrt{d}} \text{ with URM Infills} \quad (1.2)$$

$$T = 0.075H^{0.75} \text{ without URM Infills} \quad (1.3)$$

Where, T is the design natural period of the building of height H and base dimension d along the considered direction. As per IS-1893 (2016), the base shear obtained from the response spectrum method shall not be less than the base shear obtained from code provisions, if so it needs scaling accordingly. The maximum drift must not exceed 0.4% under the design base shear taking partial safety factors for all the loads as 1.0.

2.3 Modelling of RC members

In order to investigate the three dimensional response of a building it is important to adequately represent the effective behavior of RC members. The inelastic behavior of the beams and columns are modelled by concentrating nonlinearity at the ends in plastic hinge regions. ASCE-41 (2016) provides the generalized force deformation curve represented by a back-bone curve as shown in figure 1.1. Where the line AB represents the linear elastic behavior and no plastic deformation is observed in this region. At point B the section yields it is represented by the expected yield strength of the section obtained from the moment-curvature relation. The line BC represents the strain hardening and line CD represents the initial failure of the section due to spalling of concrete. The line DE represents the residual strength of member and point E represents the failure point. Also the performance levels of members namely Immediate Occupancy (IO), Life Safety (LS), Collapse Prevention (CP) is shown in figure 1.1. The

acceptance criterion for plastic rotations is considered as per ASCE-41 (2016) guidelines based on the shear and axial forces, percentage of longitudinal and transverse reinforcement. RC sections are expected to yield under seismic loading, which results in cracking of the section. The effective stiffness is considered from the provisions given in IS-1893 (2016) as shown in table 1.0

Table 2.1 Effective stiffness of RC members as per IS-1893(2016)

RC MEMBER	MOMENT OF INERTIA
BEAM	$0.35I_g$
COLUMN	$0.7I_g$

Where, I_g is the gross moment of inertia of concrete section

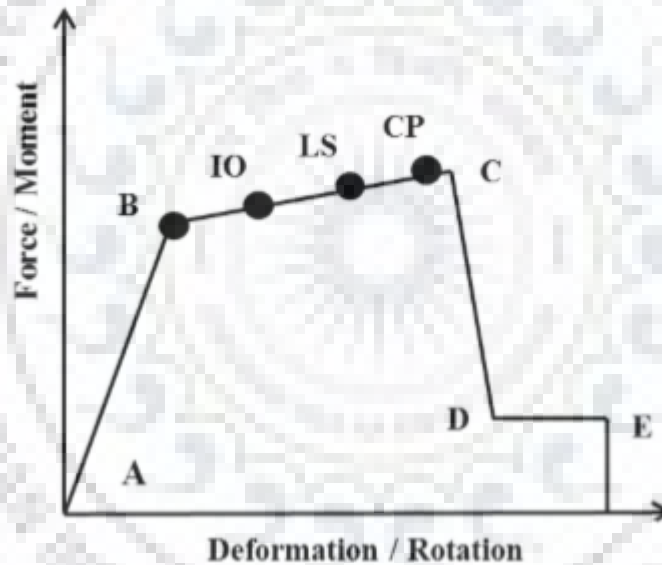


Figure 2.1 Generalised force-deformation behaviour of a typical RC member to define performance limit state under flexure as per ASCE-41 (2016)

2.4 Modelling of URM Infills

Modeling of Infills is an important step in assessment of a seismic safety of URM infilled RC frame buildings. Past experience shows that frames with infill especially nonductile concrete frames are prone to failure during an earthquake (Burton and Deierlien, (2014)). Several researches have been carried on the analytical modeling of URM Infills since 1960's. As simulation of the actual behavior of an infilled frame is a very troublesome task, because of its interaction between the infill and the frame,

different modeling techniques have been proposed in literature. Broadly, modeling of URM can be categorized in two types – Micro and Macro models. Micro modeling is based on the finite element representation thus will capture the behavior in much detailed manner. However, these are computationally complex and lengthy, whereas macro models are based on gross understanding of the behavior of Infills and therefore are able to simulate the overall behavior of Infills efficiently and quite approximately. In this project considering above mentioned points, Equivalent strut model which is the most acceptable analytical macro model in which effect of an infill is represented by a single or multiple compression only struts within the frame. In the present study each infill panels are represented by pair of diagonal struts considering the frame-infill interaction and also the cyclic loading.

2.4.1 Macro Modeling of URM Infills

Due to the very high degree of non-homogeneity and nonlinear brittle behavior of masonry, Infills resulting in computational complexity creates the need for a simplified models which can represent the strength and stiffness almost accurately. Thus this leads us to adaptation of macro modelling based analysis procedure (Haldar *et al*, 2013).

The idea of the strut models was first introduced by Polyakov (1960) based on elastic theory. Holmes in 1963 proposed that the width of the diagonal should be 1/3rd of the length of the panel. Later many researchers proposed their own models. In the present study, the width of the diagonal strut model was calculated by using the equation given in IS-1893 (2016) which is based on the work done by Smith and Carter (1969). The width is calculated by using relative stiffness of the infill and the surrounding frame. Based on IS-1893 (2016), the equivalent width of the infill is obtained as:

$$w_{ds} = 0.175\alpha_h^{-0.4}L_{ds} \quad (1.4)$$

Where

$$\alpha_h = h \left(\sqrt[4]{\frac{E_m t \sin 2\theta}{4E_f I_c h}} \right) \quad (1.5)$$

E_m = Modulus of elasticity of the URM infill

E_f = Modulus of elasticity of the frame material

I_c = The moment of inertia of the adjoining column

t = Thickness of the infill wall

h = Clear height of the URM infill wall

L_{ds} = Length of the diagonal strut

W_{ds} = Width of the strut

θ = Angle of the diagonal strut with horizontal

Generally, Infills have two prominent failure modes those are shear failure and diagonal compression failure

To model the masonry infill in non-linear static analysis, the stress strain curve of the masonry prisms were obtained from seven different specimens with combination of different grades of burnt bricks and mortar from a total of 84 specimens. An experimental study done by (Kaushik *et al*, 2007) provides the above mentioned data. In their study to capture the non-linear characteristics, compressive forces were applied on the masonry prism through a displacement controlled servo-hydraulic actuators, and the corresponding deformation were recorded using an Epsilon extensometer. The stress strain model comprises of three portions: a parabolic rising curve, a linear falling branch, and a final horizontal line at 20% stress level of masonry prism strength earlier given as “modified Kent-Park model (Priestley and Elder 1983). In the study done by (Kaushik *et al*, 2007) it has been observed that the ascending parabolic part can be represented by following non dimensional equation:

$$\frac{f_m}{f'_m} = 2 \frac{\varepsilon_m}{\varepsilon'_m} - \left(\frac{\varepsilon_m}{\varepsilon'_m} \right)^2 \quad (1.6)$$

Where f_m and ε_m are compressive stress and strain in masonry respectively, and ε'_m is the peak strain corresponding to f'_m . The parabolic curve can be extended until the curve drops to 90% of the peak compressive strength. After the point of $0.9 f'_m$ the curve is assumed straight line till the residual stress, i.e.20% of f'_m . The ε'_m value was found by regression analysis of experimental data.

$$\varepsilon'_m = C_j \frac{f'_m}{E_m^{0.7}} \{R^2 = 0.83, \sigma = 0.0001\} \quad (1.7)$$

Where C_j is factor depending upon the strength of mortar which is given by:

$$C_j = \frac{0.27}{f_j^{0.25}} \quad (1.8)$$

The descending linear curve is formed by joining $0.9 f'_m$ to $\{2\varepsilon'_m, 0.2f'_m\}$ for mortar without lime content, and to $\{2.75\varepsilon'_m, 0.2f'_m\}$ for mortar with lime. A higher failure strain in mortar with lime is because of the reason that lime increases the ductility of the masonry. Idealized stress strain curve for masonry adopted for this study is shown in figure below

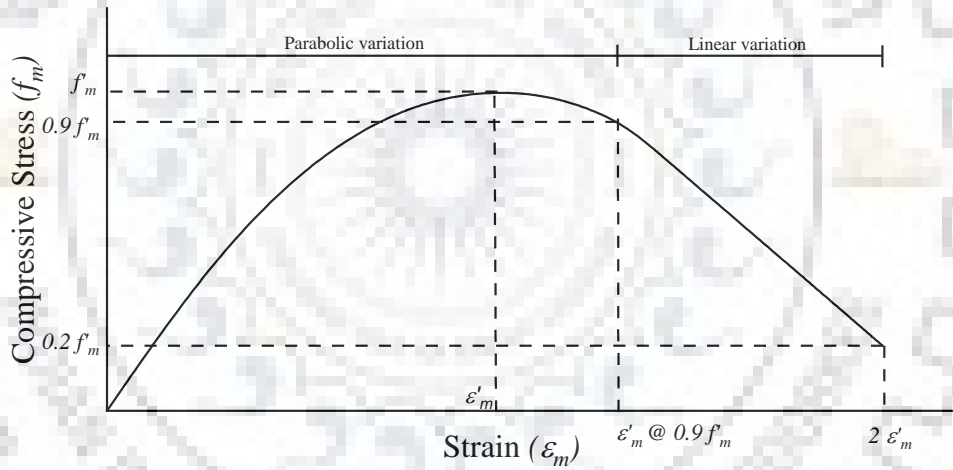


Figure 2.2 Idealized stress strain relationship for masonry (Kaushik *et al*, 2007)

2.5 Hysteretic Modelling

Hysteresis is the phenomenon of dissipation of energy through deformation. In case of nonlinear time history analysis, modelling of hysteretic behavior is important due to reverse cyclic loading and deterioration effect. To analyze the response of a structure over a range from serviceability limit states to near-collapse limit states, it is necessary to develop hysteretic models that incorporate all important factors of deterioration in strength and stiffness which contributes to response as the structure approaches collapse. Different hysteresis models are available to describe the behavior of RC

members during cyclic loading. These models differ in the amount of energy they dissipate per cycle of deformation and how the behavior of dissipating energy changes with the increase in deformation.



CHAPTER 3: MODELLING AND ANALYSIS OF BUILDING

3.1 Building Description

An architectural plan of an already existing open ground storey building is adopted. It has a slight irregular plan with maximum dimension in longitudinal and transverse direction as 18.5 m and 12.2 m respectively. The height of the building from ground level is 18.6 m. Floor to floor height for ground storey is 3.6 m while for other storeys a uniform height of 3 m is maintained. The building has 6 columns in longitudinal direction and 4 columns in transverse direction. The building is resting on medium soil in ZONE V of IS-1893 (2016). General points worth noting about the building:

- The slab thickness is 120 mm. At the ground floor no slabs have been provided only plinth beams are considered.
- External walls are 230 mm thick while as internal walls are 115 mm thick.
- Deduction for the openings are ignored while calculating the seismic load.
- In all the cases the building is considered to be fixed at the ground level.

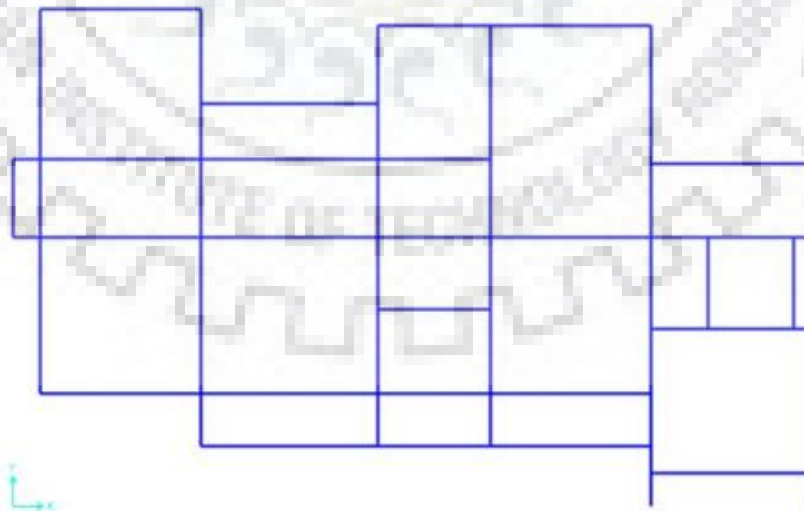


Figure 3.1 Plan of the considered building

The Dead Load (DL) and Live Load (LL) are estimated from IS-875(1987(Part 1)) and IS-875(1987(Part 2)) respectively. For the seismic design of building IS-1893 (2016) have been adopted. For design, M20 concrete and FE415 steel have been used. The strength of the masonry prism is taken 3.64 Mpa as per the strength of masonry available in India.

Table 3.1: Sizes of Beams and Columns

No.	Member	Size
1	Beam (a)	300 x 500
2	Beam (b)	230 x 500
3	Column (a)	350 x 650
4	Column (b)	350 x 830

Width of the struts were calculated from the equation provided in IS-1893 (2016) and are tabulated below

Considering the fact that buildings in India are mostly designed without the effect of masonry infill, building is first designed for earthquake and gravity loads using relevant Indian Standard codes without considering the effect of Infills. After the design, nonlinear static and dynamic analysis has been done to check performance with and without Infills.

3.2 Modelling

Three dimensional space frame model of the selected building has been done on SAP 2000. Beams and columns are modelled as 3D frame using section designer. Masonry Infills are modelled as equivalent strut compression only members. The property of masonry Infills are taken from the stress strain curve from the model adopted, and are modelled as compression only members. Since compression only is a nonlinear property it can only be applied in nonlinear analysis.

3.2.1 Inelastic Modelling

Lumped plasticity model is used in which plastic hinges are assumed to be lumped at the ends of the columns and beams. The generalized force deformation behavior is adopted from the backbone curve given in ASCE-41 (2016). To assign the plastic rotation flexural (M) and axial force-biaxial moment interaction hinges (P-M-M) hinges are assigned at a distance $L_p/2$ from the surface of beams and columns, respectively.

Where L_p is the length of plastic hinge and it can be assumed as the half of the depth of section (Park and Paulay, 1975). The flexural capacity of the columns and beams are calculated considering expected strengths of concrete and steel. The expected strength for concrete is assumed 1.5 times nominal strength and 1.25 times the minimum specified strength in case of steel ASCE 41 (2016). Mander's model for concrete has been used, the usable strain limits are 0.02 for confined concrete and 0.05 for longitudinal reinforcement in tension (ASCE-41 2016). For the URM Infills axial (P) hinges have been assigned at center of the strut, and the property is adopted from the stress strain curve is obtained from the model given by (Kaushik *et al*, 2007).

The P-M2-M3 hinges from SAP auto hinge have been validated from IS code P-M interaction curve.

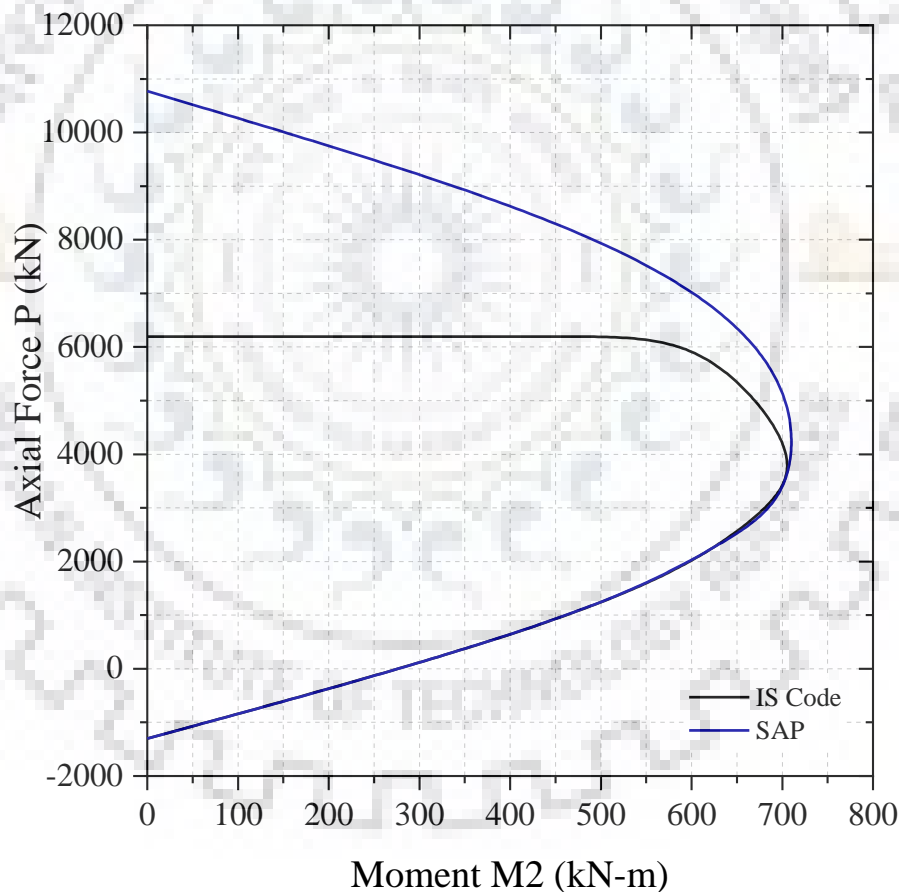


Figure 3.2 Validation of the sap auto hinge with IS-456 (2000)

3.3 Determination of Design Lateral Force

For the computation of design lateral force either modal analysis procedure or dynamic analysis can be performed. The simplest one would be equivalent static method, the

procedure. The difference between the equivalent static method and dynamic analysis method would be the magnitude of lateral force and how it is distributed over the height.(Agarwal and Shrikhande).

3.3.1 Equivalent Static Method

As stated above equivalent static method is the simplest method it requires less computational effort. The lateral force depends upon the fundamental mode period computed as per code based formula. The design base shear is first calculated as a whole and then distributed over the height based on the appropriate formulas for the type of buildings with regular mass and stiffness distribution given in IS 1893 (2016). In case of rigid diaphragm, total shear in any horizontal plane shall be distributed in the lateral load resisting members on the basis of their relative rigidity. IS-1893 (2016) gives an expression to calculate design base shear V_B along any principle direction:

$$V_B = A_h W \quad (3.1)$$

Where,

A_h = Design horizontal seismic coefficient

W = Seismic weight of the building.

$$A_h = \frac{Z I S_a}{2 R g} \quad (3.2)$$

Where, Z is the zone factor for maximum considered earthquake. The factor 2 in the denominator will reduce it from maximum considered earthquake to design based earthquake. I is the importance factor, which depends upon the functional use of the building. For the considered building, an importance factor of 1.0 has been used.

R is the response reduction factor, the use of R is to consider the inelastic characteristics in linear analysis, since it is not desirable or economical to design a building on a basis that it will remain in elastic range. A response reduction factor of 5.0 has been used for SMRF buildings IS-1893 (2016). (S_a/g) is the average response acceleration coefficient for 5% damping of the structure.

As per IS-1893 (2016) the lateral force is distributed in a parabolic form along the height of the structure by the following expression

$$Q_i = V_B \frac{W_i h_i^2}{\sum_{i=1}^n W_i h_i^2} \quad (3.3)$$

Where,

Q_i = Design lateral force at floor i

W_i = seismic weight of floor i

h_i = Height of floor i measured from base, and

n = Number of levels at which masses are located.

3.3.2 Response Spectrum Method

Response spectrum method is a linear dynamic analysis use to compute design base shear. In a response spectrum method the lateral forces calculated by considering the effect of natural vibration modes, which further depends on distribution of stiffness and mass over the height of building. IS-1893 (2016) recommends that linear dynamic analysis should be used for all the buildings other than buildings lower than 15 m in seismic zone II. It also recommends that the base shear calculated from the response spectrum method shall not be less than the one calculated from equivalent static method.

When V_B is less than \bar{V}_B , it should be scaled up by a factor $\frac{\bar{V}_B}{V_B}$. Given below is the response spectra for a medium soil as per Indian standard code.

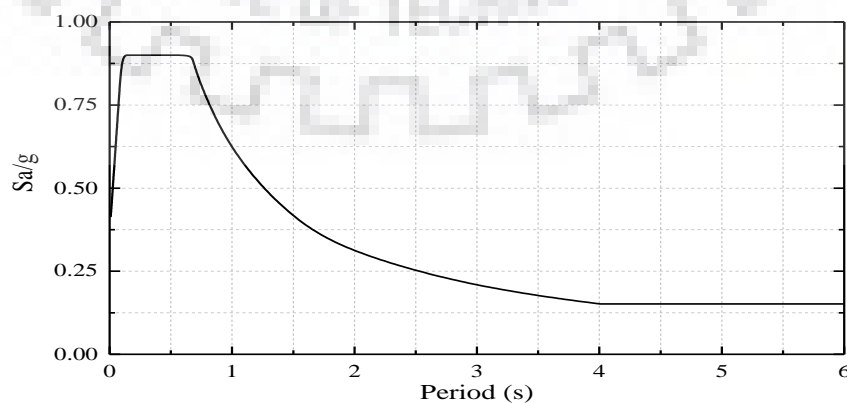


Figure 3.3 IS-1893 Part-1 (2016) spectra for Response Spectra Method

The response spectrum analysis of an irregular building is performed by 3D modelling of the structure which will represent the stiffness and mass distribution properly. Modal analysis is done to get the natural time periods and mode shapes. Number of modes to be considered is such that the modal mass participation is at least 90% of total seismic mass. To find the storey shear force (V_i) in storey i due to all the considered modes are computed by combining due to each mode either by Square Root of Sum of Squares (SRSS) and Complete Quadratic Combination (CQC) methods.

3.4 Pushover Analysis

Nonlinear static analysis or Pushover analysis is a simplified nonlinear analysis method which can give a proper insight in to the performance of a structure under lateral load. In pushover analysis lateral load applied is increased monotonically, identifying the failure modes. A pushover curve is formed which is a plot between base shear and the roof displacement. From the capacity curve obtained the inelastic response of the structure is estimated by different approaches.

CHAPTER 4: NONLINEAR DYNAMIC ANALYSIS

The most realistic nonlinear analysis is the nonlinear time history analysis for the prediction of forces and displacements in a seismic loading, it involves time step by step evaluation of the building response. In the present study, the nonlinear time history analysis has been done on both DBE and MCE level earthquakes.

4.1 Ground Motion Selection

The ground motions were selected from PEER Ground motion data base and were scaled with the target response spectra of IS-1893 (2016) for Zone V and medium soil. 11 ground motions were selected as suggested by ASCE-7 (2016). These 11 ground motions were selected for far field site with a shear wave velocity (V_{s30}) of 180-240 km. ASCE-7 (2016) the ground motions are required to scale between $2T_1$ and $0.2T_{90}$ such that their average lies above the 0.9 times the target spectrum. Where, T_1 fundamental time period and T_{90} time period at which there is at least 90% mass participation in both directions. There are two procedures available to make the grounds compatible with the target response spectrum those are: amplitude scaling and spectral matching. In the present study amplitude scaling have been adopted.

4.2 Amplitude Scaling

In amplitude scaling one entire ground motion is applied with a single scale factor such that time to time variability is preserved. For this study the mean square averaging has done between the period ranges of interest. Table 3.1 gives the detail of ground motions selected. Figure shows the combined mean spectra along with the individual ground motions.

Table 4.1 Details of ground motion records selected for NLTH analysis

Record ID	Earthquake Event	Year	Station	Magnitude	Mechanism	Vs30 (m/s)	Rupture	PGA
172	"Imperial Valley-06"	1979	"El Centro Array #1"	6.53	Strike slip	237.33	21.68	0.255
175	"Imperial Valley-06"	1979	"El Centro Array #12"	6.53	Strike slip	196.88	17.94	0.210
719	"Superstition Hills-02"	1987	"Brawley Airport"	6.54	Strike slip	208.71	17.03	0.256
728	"Superstition Hills-02"	1987	"Westmorland Fire Sta"	6.5	Strike slip	193.67	13.03	0.153
1536	"Chi-Chi_ Taiwan"	1999	"TCU110"	7.62	Reverse oblique	212.72	11.58	0.233
5249	"Chuetsu-oki_ Japan"	2007	"NIG003"	6.8	Reverse	187.36	47.45	0.326
5975	"El Mayor-Cucapah_ Mexico"	2010	"Calexico Fire Station"	7.2	Strike slip	231.23	20.46	0.221
6005	"El Mayor-Cucapah_ Mexico"	2010	"Holtville Post Office"	7.2	Strike slip	202.89	36.52	0.196
6888	"Darfield_ New Zealand"	2010	"Christchurch Cathedral College"	7	Strike slip	198	19.89	0.195
6890	"Darfield_ New Zealand"	2010	"Christchurch Cashmere High School"	7	Strike slip	204	17.64	0.189
8161	"El Mayor-Cucapah_ Mexico"	2010	"El Centro Array #12"	7.2	Strike slip	196.88	11.26	0.235

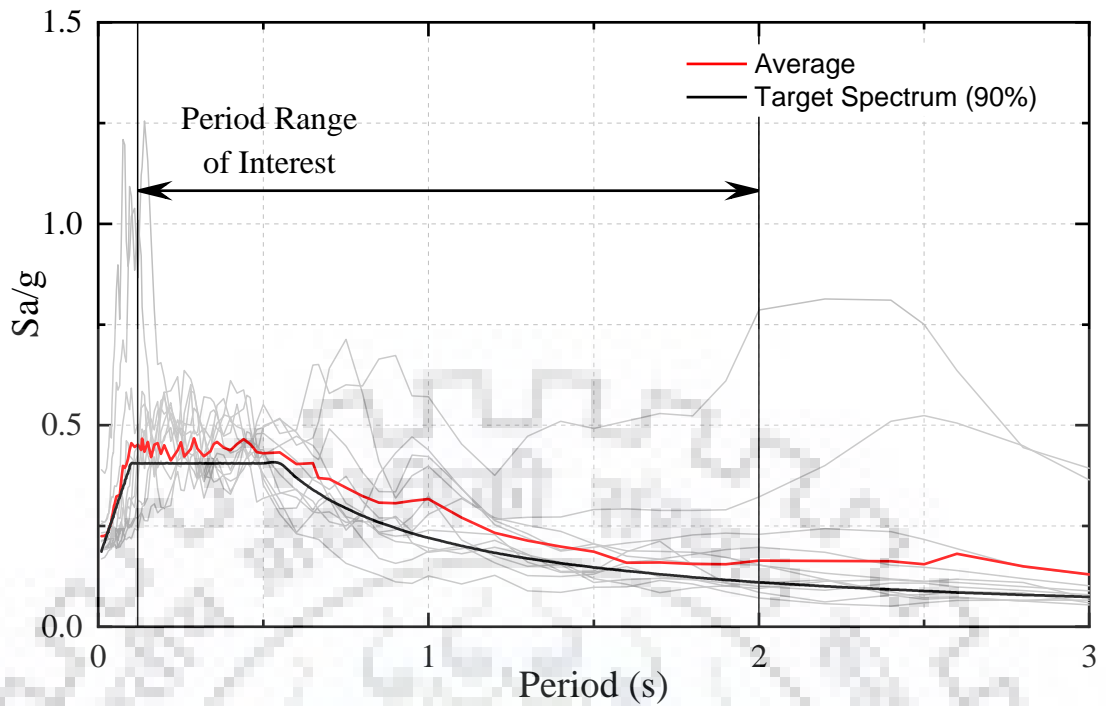


Figure 4.1 Selected ground motions

4.3 Damping

A viscous damping of 5% is considered for the building. SAP 2000 allows the use of Rayleigh damping which is a viscous damping which is basically in proportion to a linear combination of mass and stiffness. For the NLTH analysis in SAP2000 Direct-integration method has been adopted.

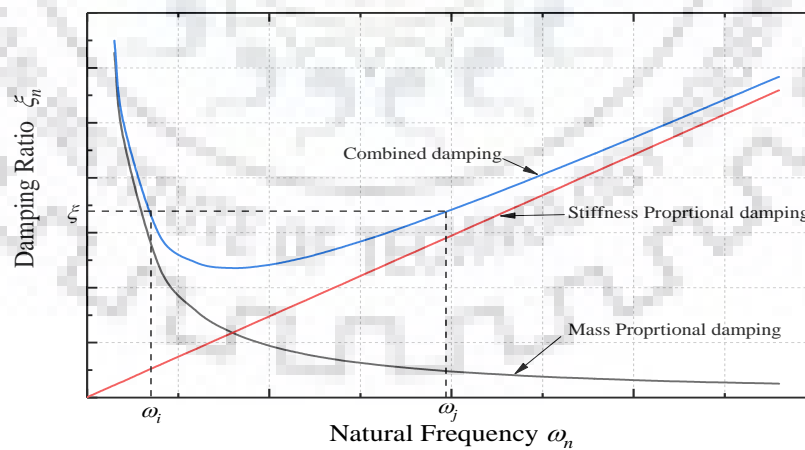


Figure 4.2 Rayleigh damping

4.4 Hysteretic Model

Isotropic Hysteresis model has been used to assess the cyclic behavior of the RC frame as well as the Masonry Infills. In an isotropic model there is an increase in strength in both direction with each cycle. The unloading takes a path parallel to the elastic line until the magnitude of action is equal to that of in reverse direction at the same amount of deformation.

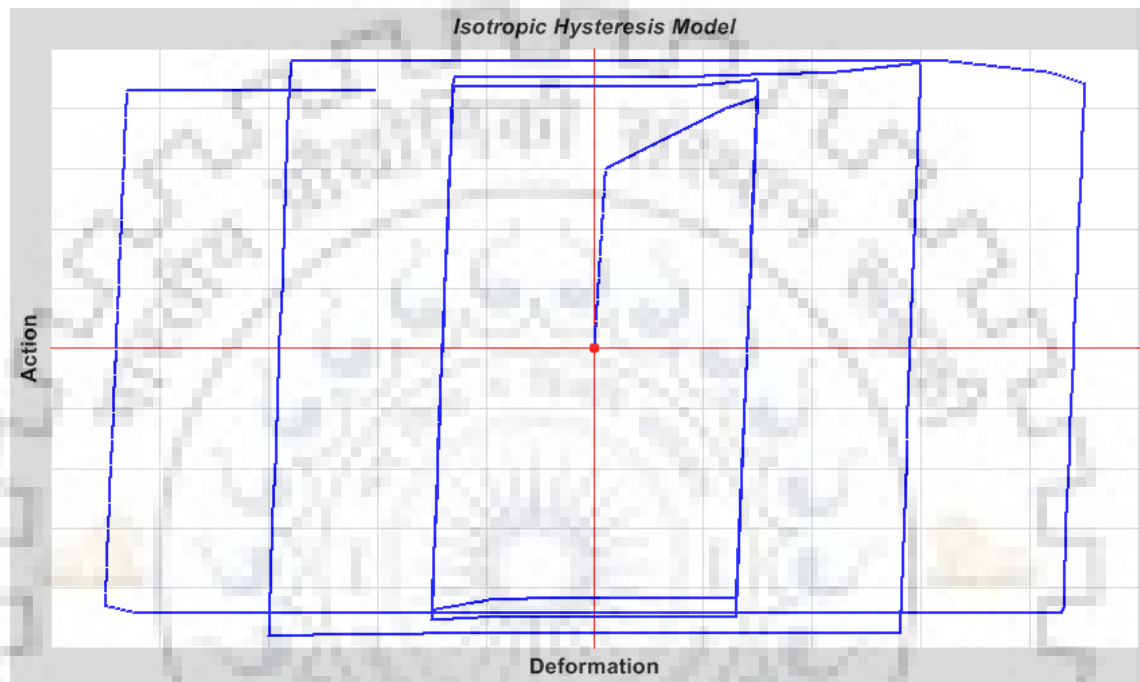


Figure 4.3 Isotropic Hysteresis modal (SAP 2000)

CHAPTER 5: RESULTS AND CONCLUSIONS

Table 5.1 Modelling and design parameters

General	Models	3D bare and infilled model
		2D infilled and bare frame in transverse and longitudinal direction
Seismic Hazard	Soil type	IS-1893 (2016) Soil Type II
	Seismic Zone	Seismic Zone V IS-1893 (2016)
Material	Concrete	$f_{ck} = 25 \text{ MPa}$
	Steel	$f_y = \text{MPa}$
	Compressive strength of infill prism	$f'_m = 3.64 \text{ MPa}$
Loading	Dead Load	Self-weight of members
		Weight of Infills
		Weight of Slabs and Floor finish
		Weight of Parapet wall 1m high and 110 mm wide
	Live load	$1.5 \text{ kN} / \text{m}^2$ on the roof area
		$3 \text{ kN} / \text{m}^2$ on all other areas
	Design load combinations	1.5 (Dead load)
		1.5 (Dead load + Live load)
		1.2 (Dead load + Live load \pm Earthquake load)
		1.5 (Dead load \pm Earthquake load)
		0.9 (Dead load \pm earthquake load)
Structural Modeling	Element models	3D frame elements for columns and Beams
		Slabs
		Strut element for Infills
	Inelastic models	Lumped plasticity model (ASCE-41)
	P-delta effect	Considered in both Pushover and NLTH analysis.

5.1 Modal Analysis

Modal analysis is a tool to understand the dynamic behavior of a structure. A structure vibrates with much higher amplitude at its resonant frequency, thus it is important to know the parameters like fundamental frequency, modal mass participation and mode shapes for a much reliable performance in dynamic loading. From the modal analysis it can be seen that as a result of modeling the infill natural time period has decreased thus made the model stiffer in lateral direction, attracting more forces. A comparison has been shown below for the different modals considered. A comparison between IS-1893 (2016) and SAP 2000 has also been made, since the code gives an empirical formula while as SAP 2000 calculates from the actual mass and stiffness.

Table 5.2 Effect of Infills on the Period of Vibration

	Frame configuration	Fundamental period (sec) (From analysis)	Design period (sec) IS-1893 (2016)
Longitudinal direction 2D	Bare	1.28	0.67
	Infilled	0.76	0.36
Transverse direction 2D	Bare	1.05	0.67
	Infilled	0.63	0.48
3D	Bare	1.246	0.67
	Infilled	0.84	-

Modal mass participation provides the idea for judging the significance of that particular mode. Modes with relatively higher mass participation can be easily vibrated by the base acceleration. Modes with less mass participation cannot be easily excited in that manner.

Table 5.3 Modal mass participation in fundamental mode of vibration

	Bare Frame	Infilled Frame
Transverse 2D	95	98.8
Longitudinal 2D	96	98
3D	81	93

Figure 5.1 and 5.2 shows the mode shapes in the first three modes of vibration for bare and infilled models.

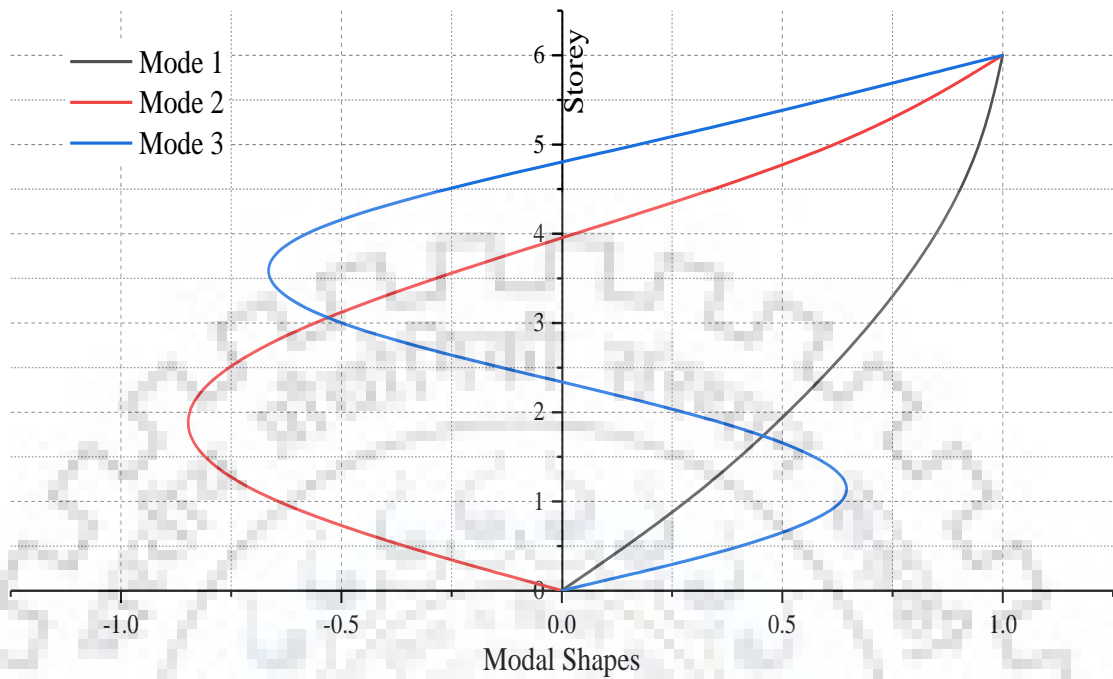


Figure 5.1 First three mode shapes for the Bare frame in transverse direction

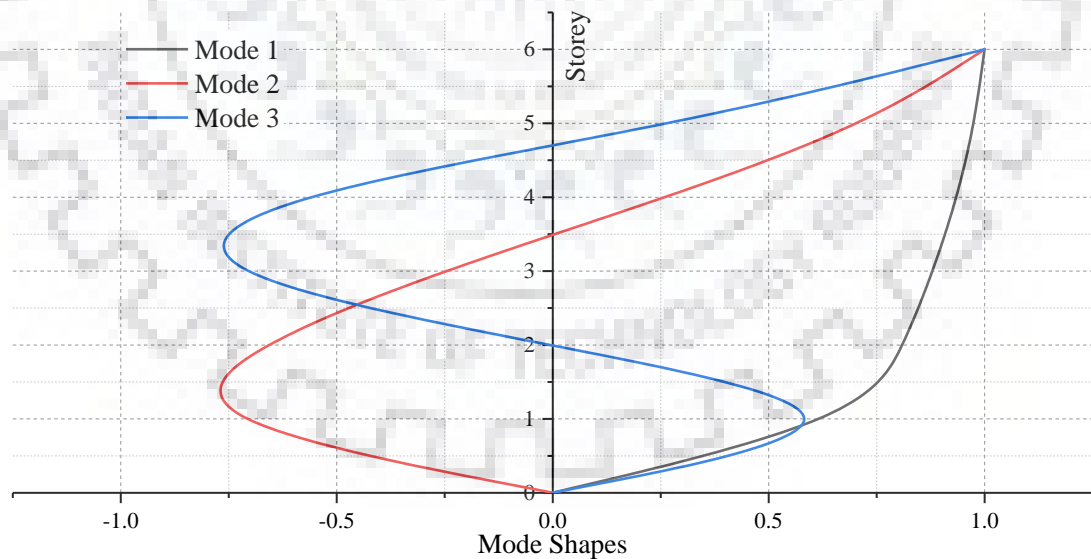


Figure 5.2 First three mode shapes for the Infilled frame in transverse direction

5.2 Base Shear

Base shear is the maximum expected lateral force at the base of a structure. It is calculated in each models with and without considering the Infills. As per IS-1893

(2016) the base shear calculated from response spectrum analysis should not be lesser than one calculated in case of equivalent static method. When it is lesser a correction factor of \bar{V}_B / V_B is applied.

Table 5.4 Base Shear and Correction factor bare frame

Case		\bar{V}_B (kN)	V_B (kN)	$\frac{\bar{V}_B}{V_B}$
Transverse 2D		75.9	45.06	1.68
Longitudinal		90	52.34	1.71
3D	X	667.5	398	1.68
	Y	685.6	339	2.02

In case of the Infills since the ‘compression only’ property can only be used in nonlinear analysis, base shear is only calculated from equivalent static method by applying the compression only struts in one direction.

Table 5.5 Base Shear comparison between bare and infilled frame.

Case	Bare Frame (kN)	Infilled (kN)
Transverse	75.9	127.9
Longitudinal	90	153.08

There is a significant increase in base shear due to the infilled since stiffer the structure more the force it will attract.

5.3 Stiffness Variation due to the Infills

Since the building considered is an open ground storey the check for soft storey is done. As per IS -1893 (2016) the storey stiffness in any storey should not be less than 70 % percent of that in storey above.

Table 5.6 Variation of stiffness due to Infills

Storey	Stiffness (kN/m)	Ratio
Open ground storey	47619.05	0.41
First storey	114508.2	

Since the ratio is less than 80% it's a soft storey, further its performance will be checked in nonlinear static and dynamic analysis. And a design philosophy will be discussed to cater this problem.

5.4 Design Forces

The building was designed for the response spectrum analysis with scaled base shear. Designing and detailing was done for SMRF building without the masonry Infills. Design critical combination was COMB 4.

Table 5.7 Design forces in ground storey columns in transverse direction.

Member	Design Pu (kN)	Design Mu(kN-m)	Design Vu (kN)
Column 1	326.102	-79.393	40.7
Column 2	511.526	-53.425	18.8
Column 3	574.134	149.557	83.569
Column 4	606.083	134.891	73.706

Table 5.8 Design forces for ground storey columns in longitudinal direction.

Member	Design Pu (kN)	Design Mu(kN-m)	Design Vu (kN)
Column 1	509.086	-15.46	5.154
Column 2	789.36	57.778	28.656
Column 3	731.102	14.622	2.806
Column 4	605.120	62.169	32.350
Column 5	1376.815	38.39	17.177

5.5 Storey Displacement and Inter Storey Drift Ratio

Storey displacement will give the displacement of that storey with respect to the ground while as Inter storey drift will give the ratio of difference between displacements of two consecutive floors to their height. Storey displacement has a very important significance

since the design has to be so done that it will accommodate the storey drifts taking in consideration that the masonry wall will not crack and fall. Figure 4.3 and 4.4 shows the absolute roof displacement with and without Infills under linear static analysis. Infilled frame has a lesser storey displacement. For the infilled frame after the first storey the displacement is very less with height showing that infilled part is acting as one stiff body, while as for bare frame it is increasing throughout.

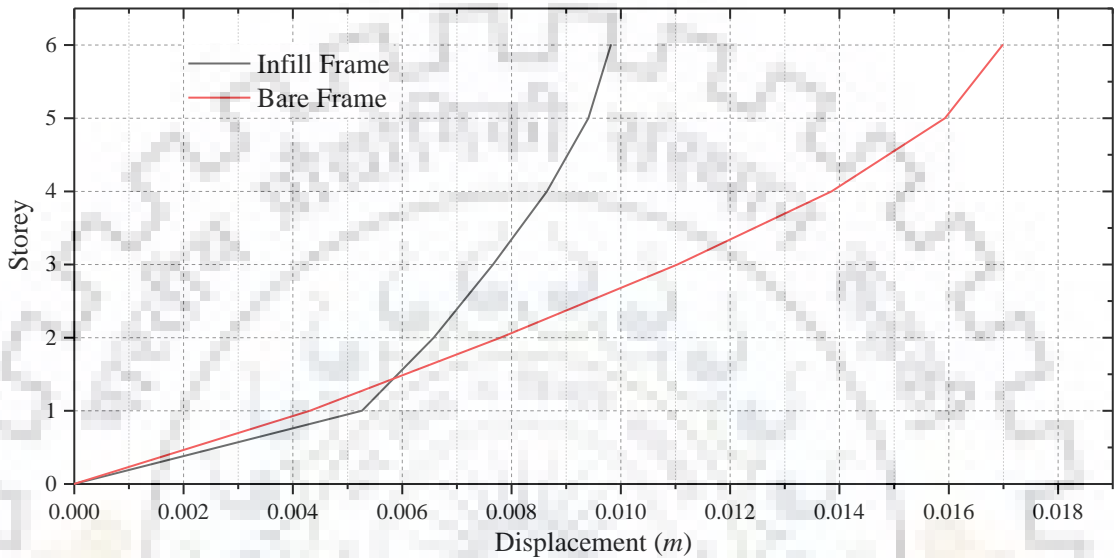


Figure 5.3 Comparison of roof displacement for bare and infilled frame under static condition in transverse direction

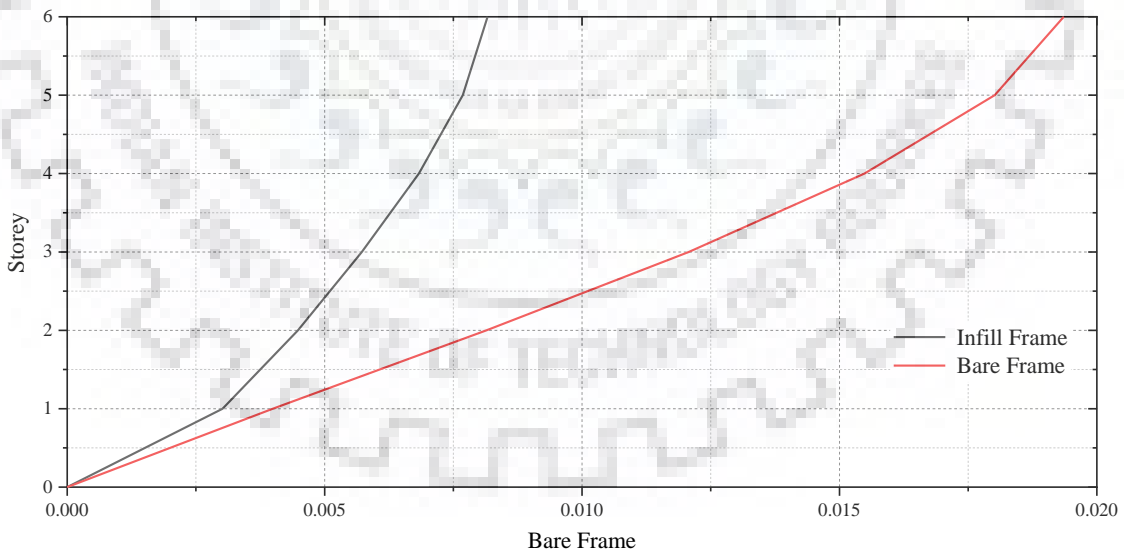


Figure 5.4 Comparison of roof displacement for bare and infilled frame under static condition in longitudinal direction

Figure 5.5 and 5.6 shows the inter-storey drift ratio for bare and infilled frames in transverse and longitudinal direction. For the bare frame inter-storey drift ratio is highest at the first storey and it gradually decreases but in case of infilled frame it is

very high at the first storey and there is a steep decrease at second storey after which change in IDR is very less for the fact that it is stiff after wards. As per IS-1893 (2016) the inter-storey drift ratio should be limited to 0.4 % of height for linear condition.

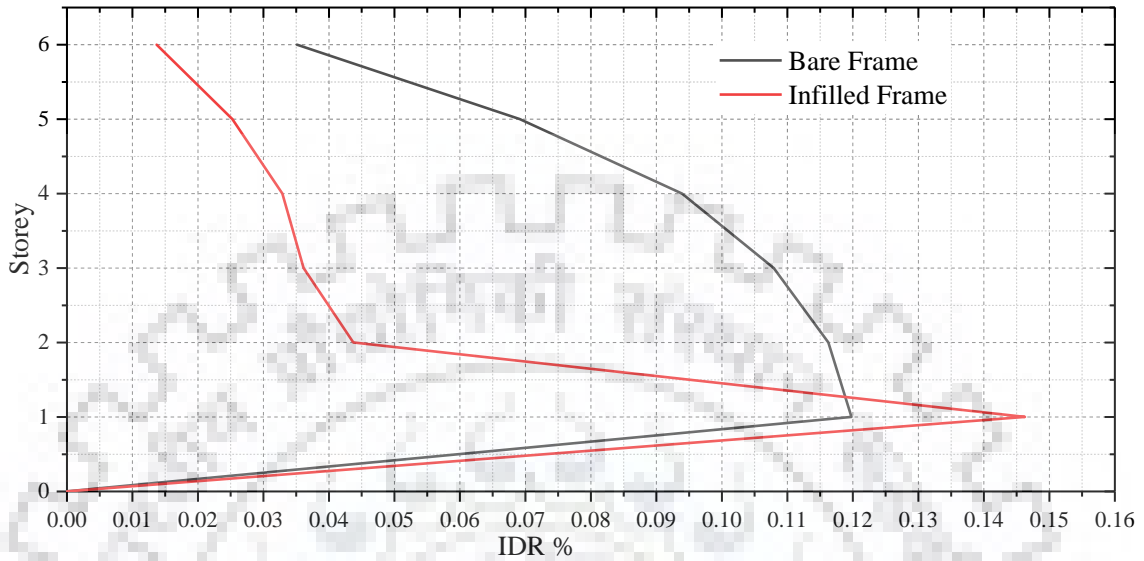


Figure 5.5 Inter Storey Drift ratio in transverse direction in case of linear static method

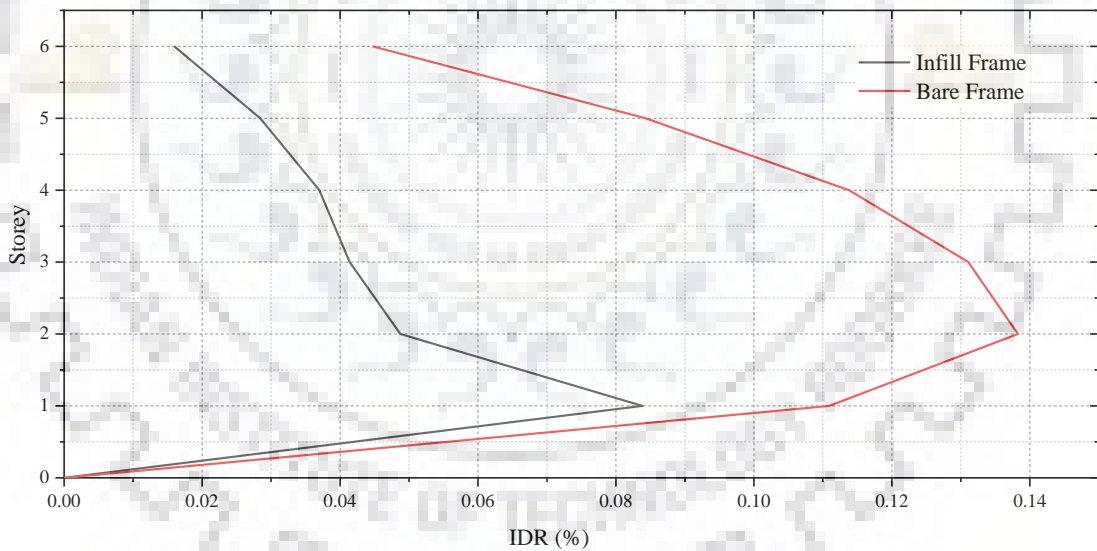


Figure 5.6 Inter Storey Drift ratio in longitudinal direction in case of linear static method

5.6 Pushover Analysis

Pushover analysis for the models has been done for the corresponding fundamental modes and the comparison is shown for the bare frame and infilled frame in figure 4.8 and 4.9.

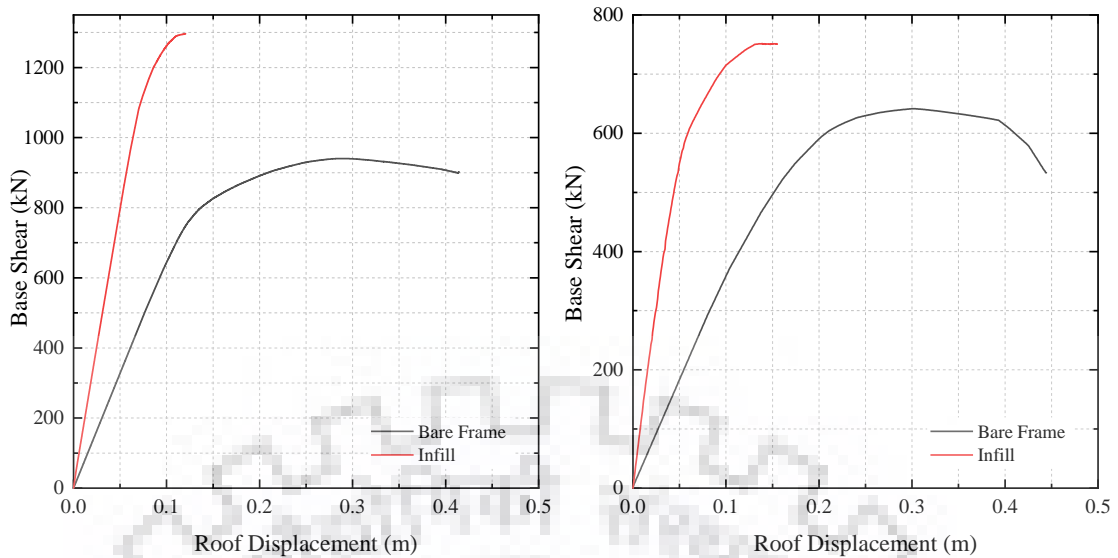


Figure 5.7 Comparison of pushover curve in (a) longitudinal and (b) transverse direction for Case 1

The comparison shows that the strength has increased in case of infilled frame but the ductility has drastically reduced, stating that the Infills give higher stiffness to the building.

Pattern of formation of hinges from figure 4.9 and 4.10 show that hinges are first developing in the infill struts and then propagates in the ground storey columns until it forms the mechanism in case of infilled frame, while as in bare frame it is propagating from the ground storey columns to the first storey beams and so on. In infilled frame pattern of hinge formation is depicting the soft storey mechanism. Thus the ground storey columns are very much vulnerable for an earthquake.

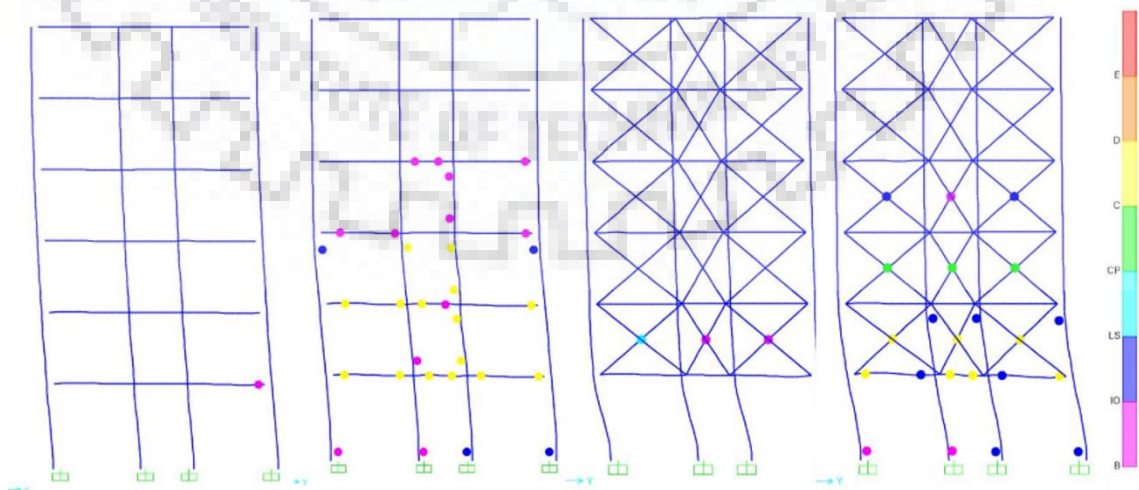


Figure 5.8 Hinge formation pattern in pushover transverse direction

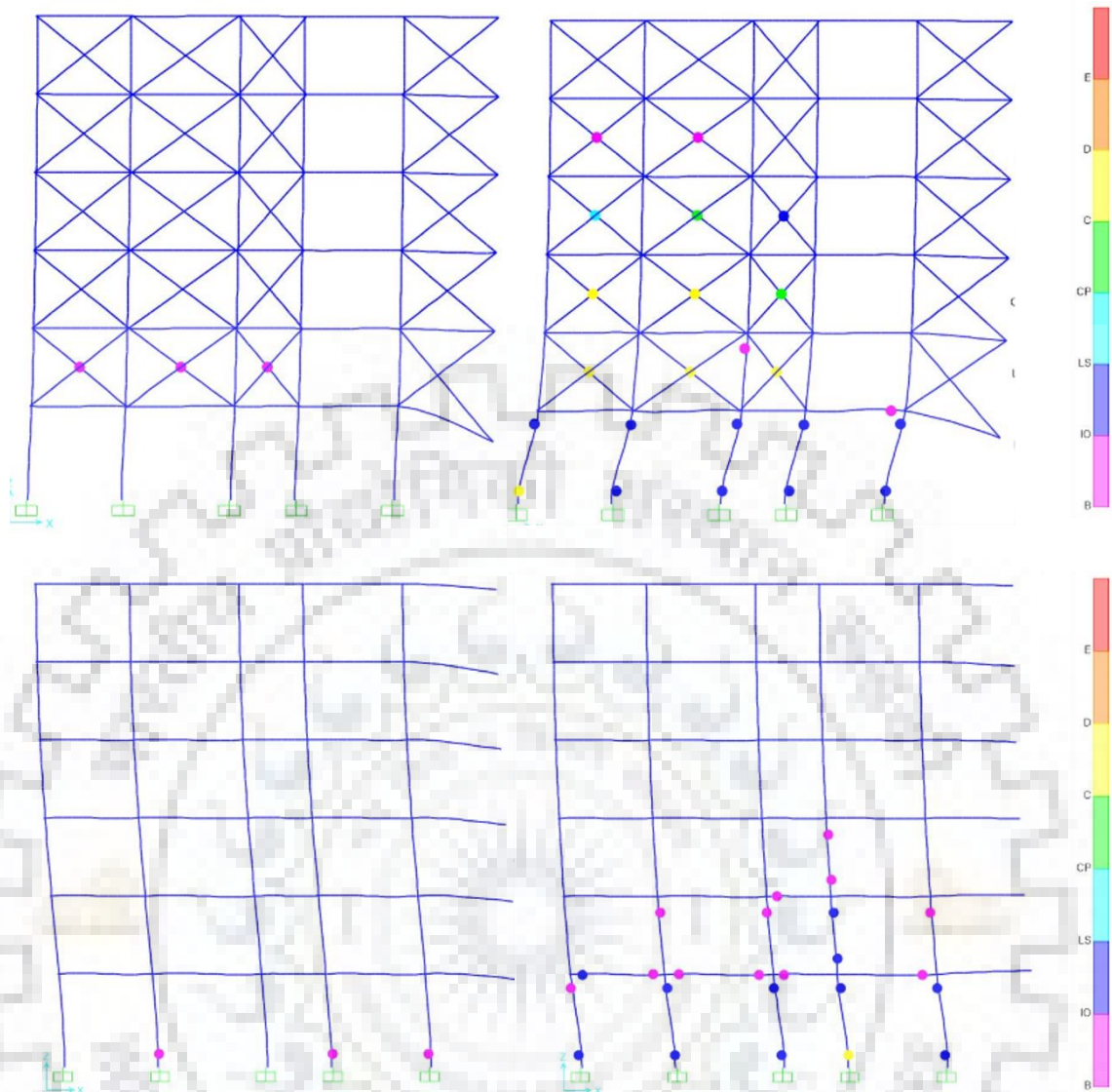


Figure 5.9 Hinge formation pattern in pushover analysis longitudinal direction

5.7 Time History Analysis

5.7.1 Base Shear

Base shears of the building in both the direction due to nonlinear history analysis have been tabulated below.

Table 5.9 Base Shear for transverse frame with and without Infills in case of Nonlinear Time History analysis

Time History	Base Shear (kN)			
	Bare Frame		Infilled Frame	
	max	min	max	min
TH 172	297.042	-331.497	274.42	-374.337
TH 175	437.827	-421.467	470.177	-416.352
TH 719	324.49	-320.228	466.724	-477.364
TH 728	352.349	-327.337	479.518	-480.531
TH 1536	538.564	-515.965	574.055	-593.789
TH 5249	166.322	-140.936	270.807	-269.711
TH 5975	440.138	-368.55	605.965	-537.362
TH 6005	315.92	-328.037	364.443	-417.935
TH 6888	429.131	-411.052	567.763	-558.492
TH 6890	447.471	-428.974	551.668	-536.591
TH 8161	433.654	-422.449	525.013	-555.839
Average	380.2644	-365.136	468.2321	-474.391

Table 5.10 Base Shear for longitudinal frame with and without Infills in case of Nonlinear Time History analysis

Time History	Base Shear (kN)			
	Bare Frame		Infilled Frame	
	max	min	max	min
TH 172	272.707	-334.119	271.558	-335.833
TH 175	461.588	-444.186	437.296	-352.209
TH 719	324.932	-304.192	387.644	-400.311
TH 728	364.895	-322.785	405.573	-430.125
TH 1536	564.942	-558.6	575.701	-686.568
TH 5249	183.746	-188.516	207.079	-226.167
TH 5975	459.759	-352.664	597.736	-536.405
TH 6005	346.862	-337.47	329.163	-360.417
TH 6888	436.64	-431.846	580.458	-619.965
TH 6890	479.207	-476.281	495.836	-504.354
TH 8161	461.531	-431.094	484.853	-577.925
Average	396.0735	-380.159	433.8997	-457.298

The results again shows that there is significant increase in base shear for the infilled frame, due to the fact that it the stiffness has increased.

5.7.2 Storey Displacement and Inter Storey Drift Ratio

Nonlinear time history analysis is the most accurate ways of assessing the performance of the structure in dynamic loading. Inter-storey drift ratio would be one of the parameters by which we can compare the performance. The average displacement of all the 11 time history are plotted against the no. of storey.

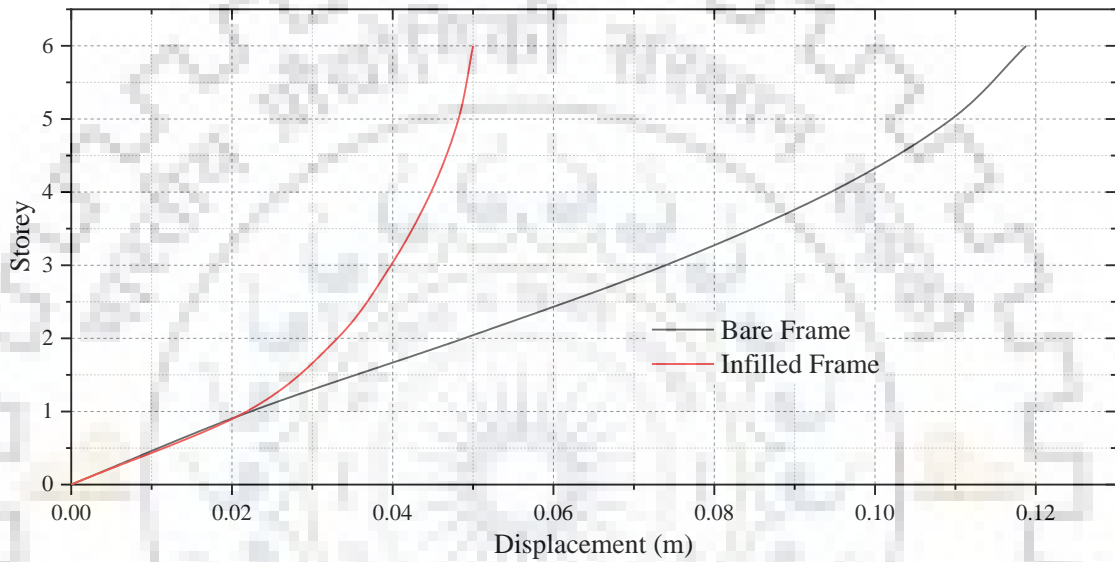


Figure 5.10 Comparison of roof displacement in transverse direction with and without Infills in NLTH analysis

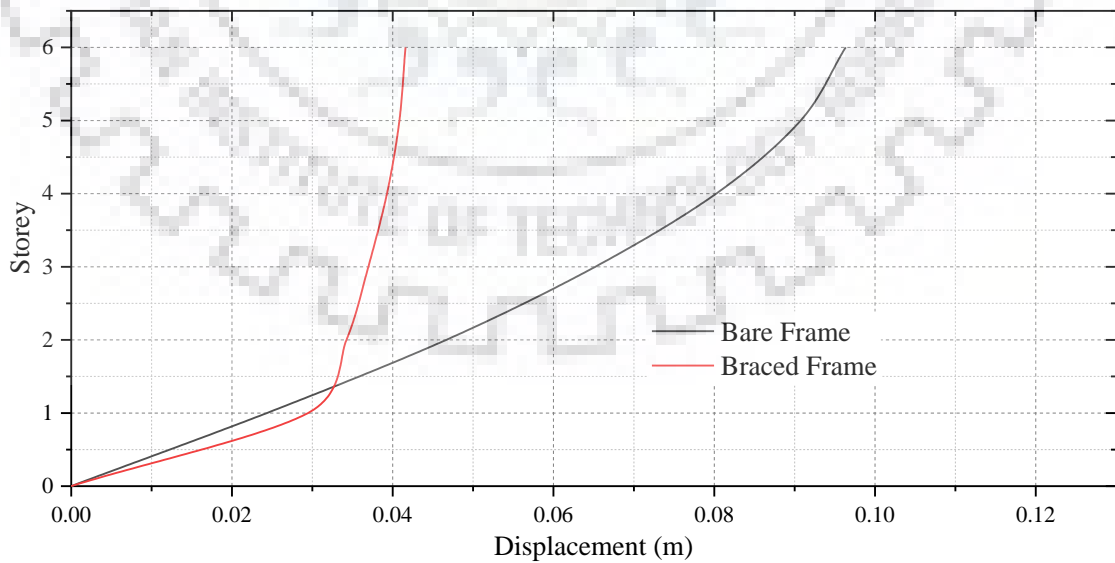


Figure 5.11 Comparison of roof displacement in longitudinal direction with and without Infills in NLTH analysis

Figure 4.11 and 4.12 gives a comparison of roof displacement and it could be seen that the displacement at the first storey is very close to displacement at the roof. The infill portion is acting as one whole portion.

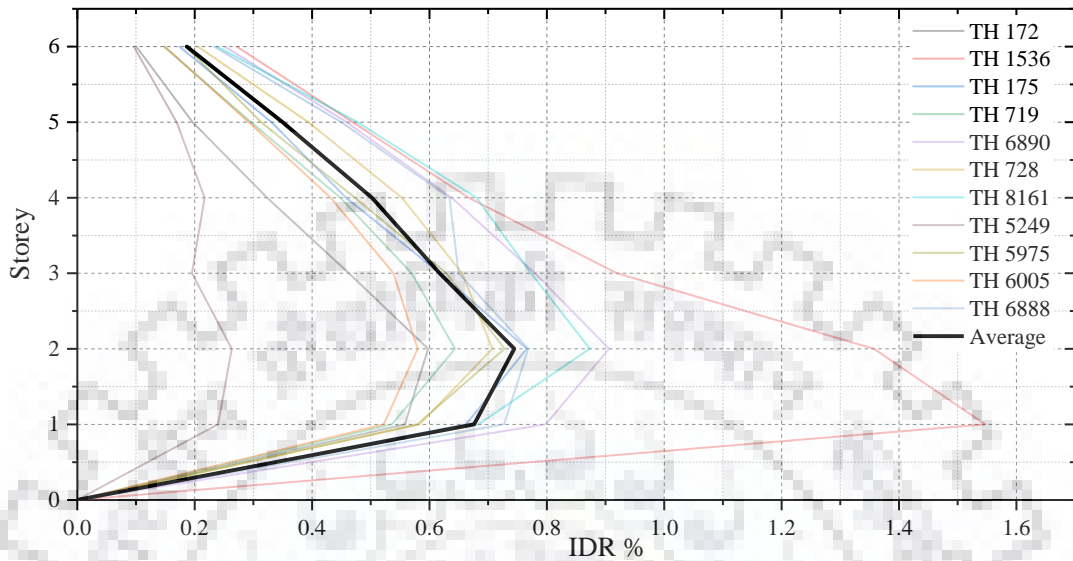


Figure 5.12 Inter-storey drift ratio for the Case 1 bare frame in transverse direction

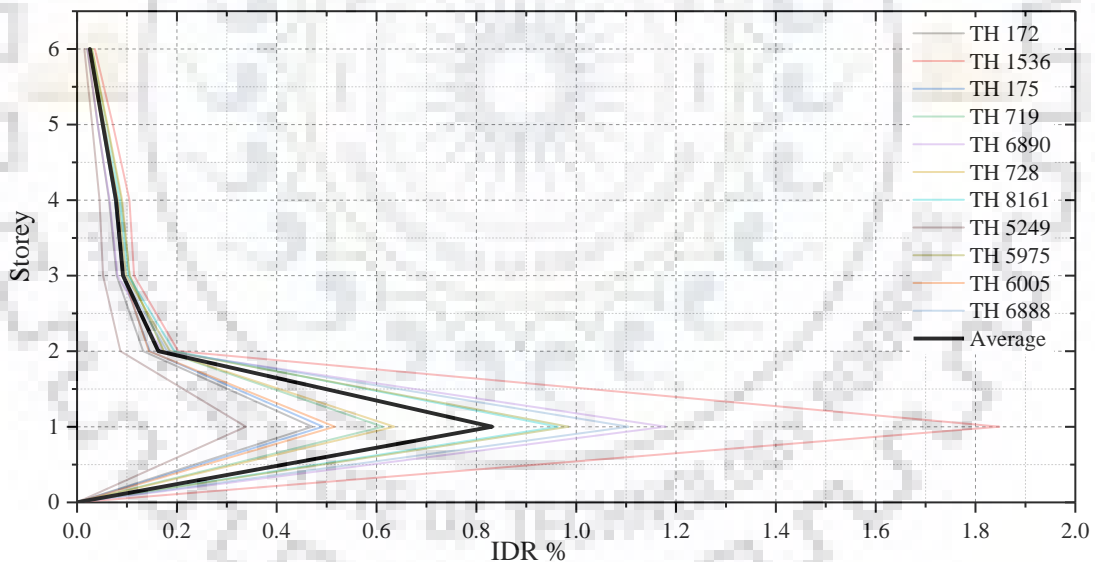


Figure 5.13 Inter-storey drift ratio for Case 1 infilled in transverse direction

In Figure 4.13 and 4.14 the inter-storey drift ratio for infilled and bare frame has been plotted against the storey. It can be seen that how because of the soft storey the drift at the first storey is very high as compared to the above infilled storeys. Similarly the same has been plotted in longitudinal direction in Figure 4.15 and 4.16.

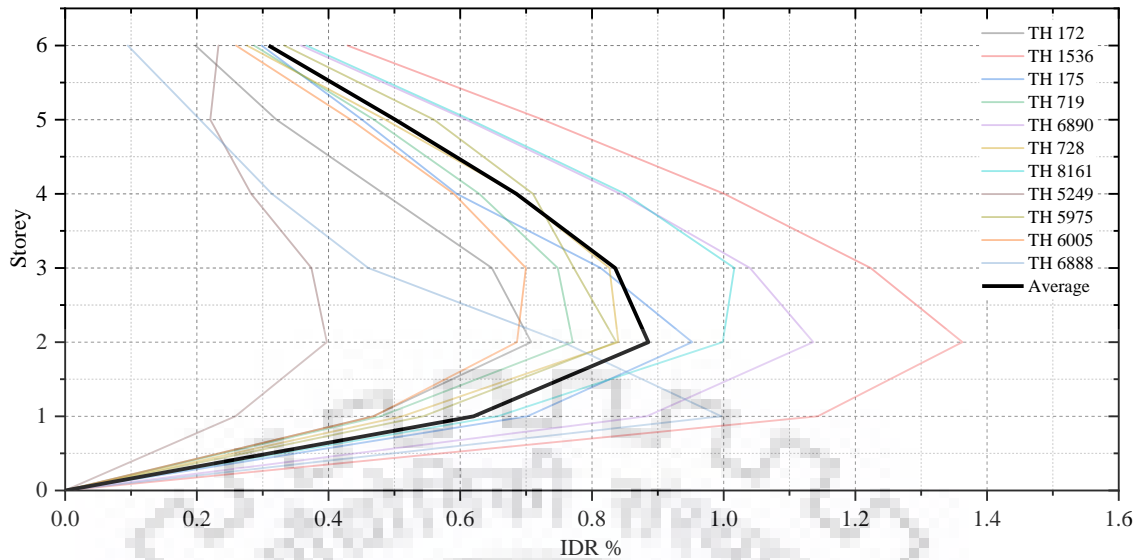


Figure 5.14 Inter-storey drift ratio for the Case 1 bare frame along longitudinal direction

The average of inter-storey drift ratio is maximum at the 2nd storey and it reduces along the height.

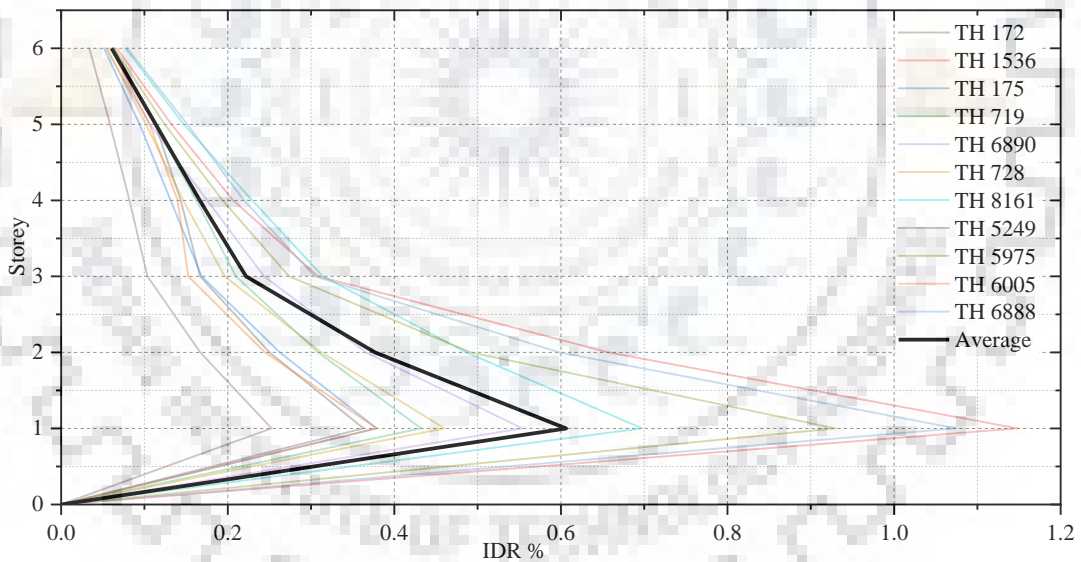


Figure 5.15 Inter-storey drift ratio for the Case 1 Infilled frame along longitudinal direction

The IDR % in transverse can be justified in a way that since building is having lesser time period will attract higher forces. The pattern shows a very high drift ratio at the first storey. It can be almost concluded that the ground storey columns are subjected to higher forces.

The hinge formation pattern has been studied for the considered building in both the directions. Pattern for only two ground motions have been shown since the pattern is very much similar in all the cases.

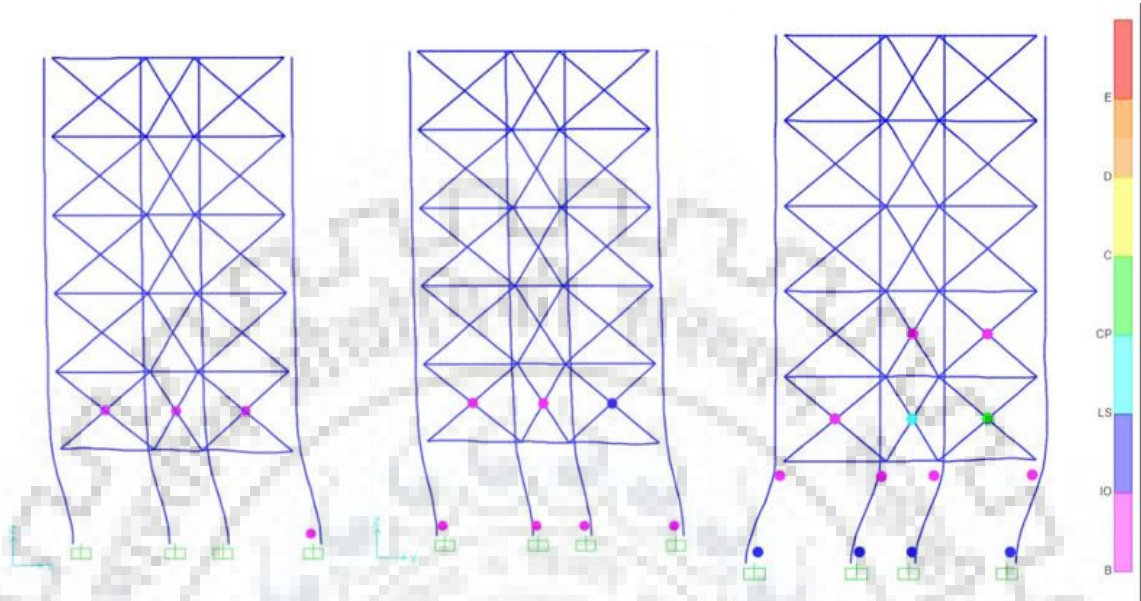


Figure 5.16 Hinge formation pattern for Case 1 infilled frame

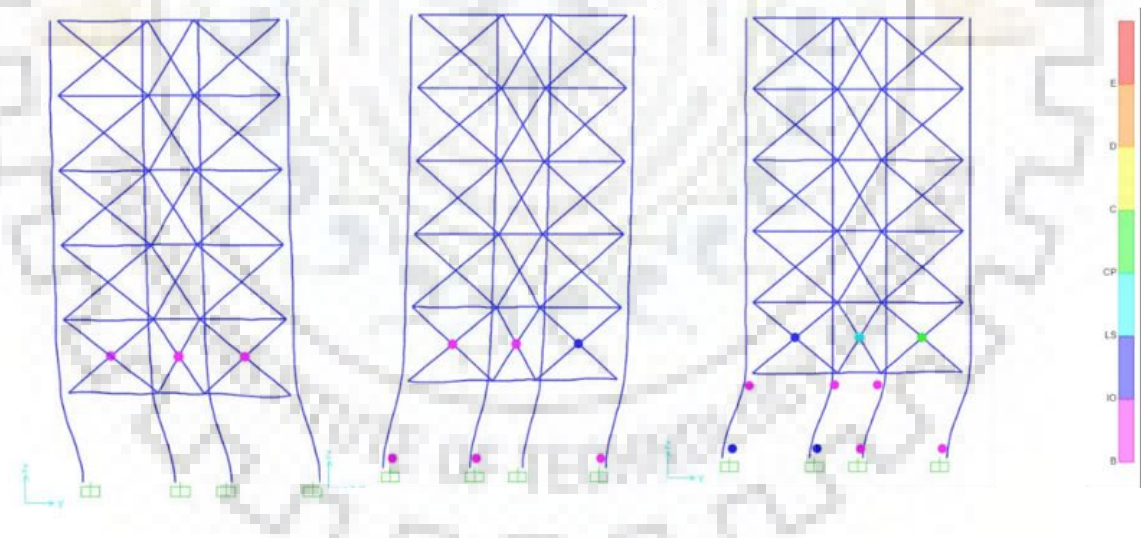


Figure 5.17 Hinge formation pattern for Case 1 infilled frame

In the first case the hinges started forming in the infill struts and later started propagating in the ground storey columns leading to the formation of a failure mechanism.

5.8 Design Cases

To improve the performance of the building considered the ground storey (soft storey) columns are designed for higher forces in static analysis as discussed earlier and each of the models are subjected to pushover and time history analysis and responses were noted.

Following three cases are considered for this study

- Case 1: Forces taken for design as per the critical combination from Response Spectrum analysis.
- Case 2: Double the forces from Case 1
- Case 3: 4 times the forces from Case 1.

The performance for the case 1 design has already been discussed earlier. After designing the ground storey columns for Case 1 and Case 2 the design reinforcement and column sizes are tabulated in Table 4.11 and 4.12.

Table 5.11 Column sizes and rebar % for different cases of design along transverse direction

Column No.	Case 1		Case 2		Case 3	
	Column size(mxm)	Rebar %	Column size(mxm)	Rebar %	Column size(mxm)	Rebar %
Column 1	0.35x0.65	0.8	0.35x0.65	1.9	0.4x0.75	4
Column 2	0.35x0.65	0.8	0.35x0.65	1.9	0.4x0.75	4
Column 3	0.35x0.65	0.8	0.35x0.65	1.9	0.4x0.75	4
Column 4	0.35x0.65	0.8	0.35x0.65	1.9	0.4x0.75	4

Table 5.12 Column sizes and rebar % for different cases of design along longitudinal direction

Column No.	Case 1		Case 2		Case 3	
	Column size(mxm)	Rebar %	Column size(mxm)	Rebar %	Column size(mxm)	Rebar %
Column 1	0.35x0.65	0.8	0.35x0.65	1.39	0.4x0.75	4
Column 2	0.35x0.65	0.8	0.35x0.65	1.39	0.4x0.75	4
Column 3	0.35x0.65	0.8	0.35x0.65	1.39	0.4x0.75	4
Column 4	0.35x0.65	0.8	0.35x0.65	1.39	0.4x0.75	4
Column 5	0.35x0.65	0.8	0.35x0.65	1.39	0.4x0.75	4

5.8.1 Base Shear

The fundamental time period and base shear obtained from linear static analysis for all three cases have been tabulated

Table 5.13 Base shear for all the three cases in linear static case

Direction	Case 1		Case 2		Case 3	
	Fundamental Period (sec)	Base shear (kN)	Fundamental Period (sec)	Base shear (kN)	Fundamental Period (sec)	Base shear (kN)
Transverse	0.63	127.9	0.587	135.9	0.5	148
Longitudinal	0.76	153	0.7	160.	0.657	177.837

5.8.2 Pushover Analysis

Pushover analysis has been done for the infilled frame for all the three different cases and the comparison has been plotted below

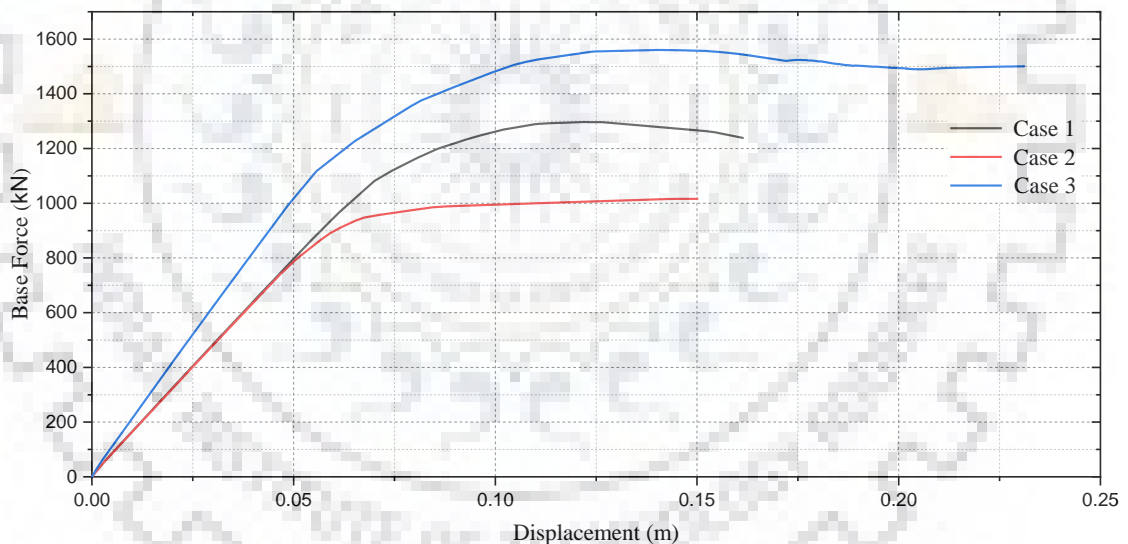


Figure 5.18 Comparison of capacity curve for all the three cases along transverse direction

From the above figures, it can be observed that as the building is design for higher forces, there is an increase in the base shear capacity of the structure. It can also be seen that ductility capacity as well has increased along both the longitudinal and transverse directions. From this we can conclude that designing for higher forces only for the soft storey can increase the strength and ductility capacity of the structure. In Figure 5.19

and Figure 5.2. The hinge formation pattern has been shown for both longitudinal and transverse direction.

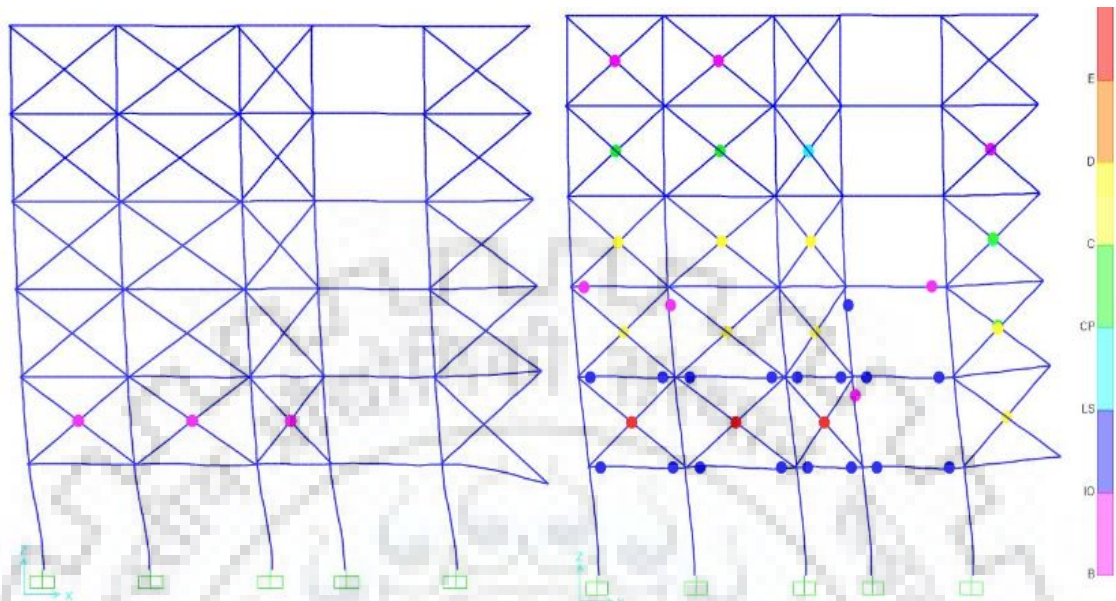


Figure 5.19 Hinge formation pattern for Case 3 in pushover analysis along the longitudinal direction

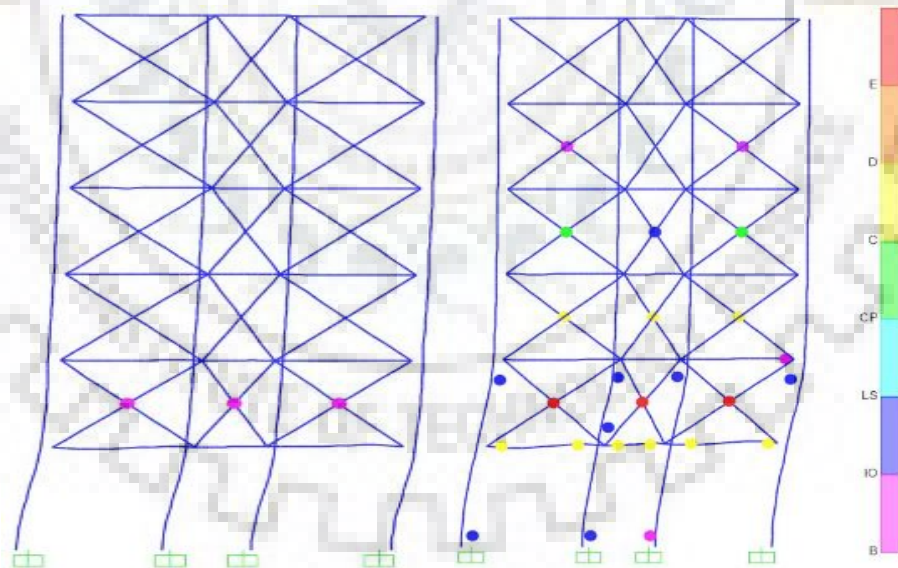


Figure 5.20 Hinge formation pattern for Case 3 in pushover analysis along the transverse direction

Average Base shear obtained from the nonlinear time history analysis for all the three cases have been tabulated in Table 4.14 and table 4.15 in transverse and longitudinal direction.

Table 5.14 Nonlinear Time History Base shear for different cases in transverse direction

Base shear (kN)	Case 1		Case 2		Case 3	
	Max	Min	Max	Min	Max	Min
TH 172	274.42	-374.337	288.446	-366.999	512.065	-799.997
TH 175	470.177	-416.352	540.726	-439.483	466.314	-376.922
TH 719	466.724	-477.364	467.845	-441.748	639.193	-651.196
TH 728	479.518	-480.531	416.644	-456.212	476.026	-532.114
TH 1536	574.055	-593.789	618.636	-726.065	659.113	-760.235
TH 5249	270.807	-269.711	253.518	-249.905	415.693	-728.866
TH 5975	605.965	-537.362	935.126	-805.968	817.892	-771.696
TH 6005	364.443	-417.935	437.963	-430.294	559.358	-799.997
TH 6888	567.763	-558.492	699.721	-663.315	672.402	-376.922
TH 6890	551.668	-536.591	770.505	-730.137	752.848	-651.196
TH 8161	525.013	-555.839	666.104	-787.78	682.678	-532.114
Average	468.2321	-474.391	554.1122	-554.355	604.87	-634.66

The base shear has significantly increased from case 1 to case 3 by 1.3 times its due to the fact that with the increase in stiffness building is attracting more forces similarly the base shear in longitudinal direction has also been tabulated in Table 5.15.

Table 5.15 Nonlinear Time History Base shear for different cases in longitudinal direction

Base shear (kN)	Case 1		Case 2		Case 3	
	Max	Min	Max	Min	Max	Min
TH 172	271.558	-335.833	301.165	-385.588	498.87	-577.447
TH 175	437.296	-352.209	502.676	-448.293	690.489	-511.688
TH 719	387.644	-400.311	445.992	-433.546	564.506	-560.795
TH 728	405.573	-430.125	372.978	-429.084	662.750	-672.050
TH 1536	575.701	-686.568	536.068	-713.843	1046.007	-1190.955
TH 5249	207.079	-226.167	250.27	-243.833	285.229	-309.679
TH 5975	597.736	-536.405	891.131	-727.257	860.875	-838.978
TH 6005	329.163	-360.417	462.735	-449.179	473.766	-603.314
TH 6888	580.458	-619.965	661.968	-595.673	1147.827	-1231.618
TH 6890	495.836	-504.354	670.577	-621.297	924.741	-906.696
TH 8161	484.853	-577.925	612.477	-744.630	761.167	-821.503
Average	433.899	-457.298	518.912	-526.566	719.657	-747.702

The increase in base shear from case 1 to case 3 has increased by 1.6 times it is due the fact that the stiffness has increased and thus the structural will attract higher forces. The inter-storey drift ratio for the transverse and longitudinal direction has also been plotted in Figure 5.21 and Figure 5.22. The comparison shows the amount of improvement in drift and hinges formation

Inter Storey Drift Ratio

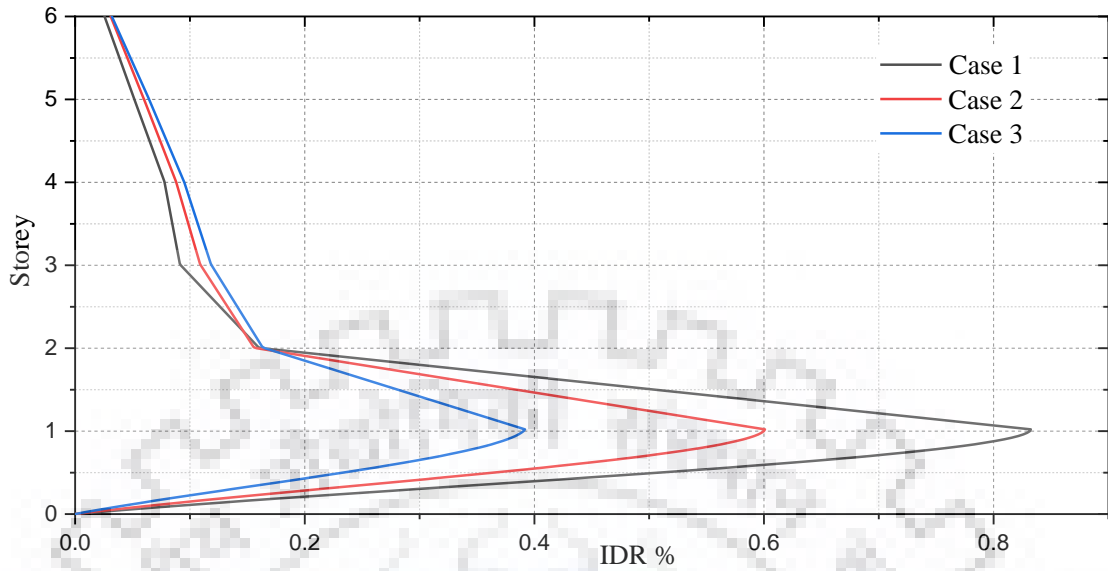


Figure 5.21 Comparison of IDR for three cases in Nonlinear Time History analysis along the transverse direction

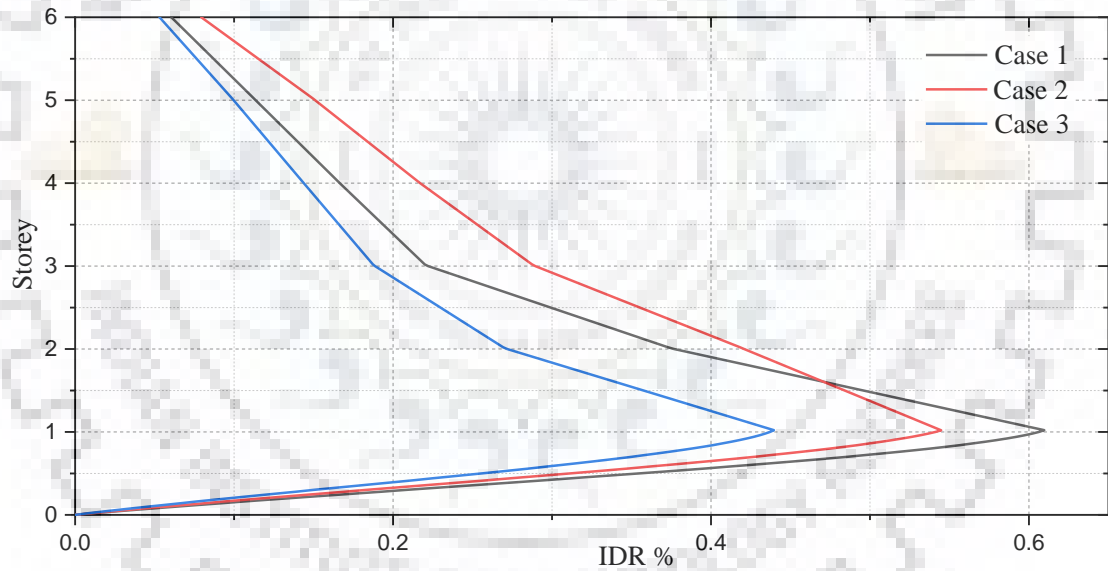


Figure 5.22 Comparison of IDR for three cases in Nonlinear Time History analysis along longitudinal direction

From the above figures it can be observed that the Inter-storey drift ratio has been reduced from 0.8 to 0.4 % in transverse direction and from 0.6 to 0.4 % in longitudinal direction. Thus, designing just the soft storey columns for higher forces can significantly increase the soft storey stiffness and decrease the Inter-storey drift ratio.

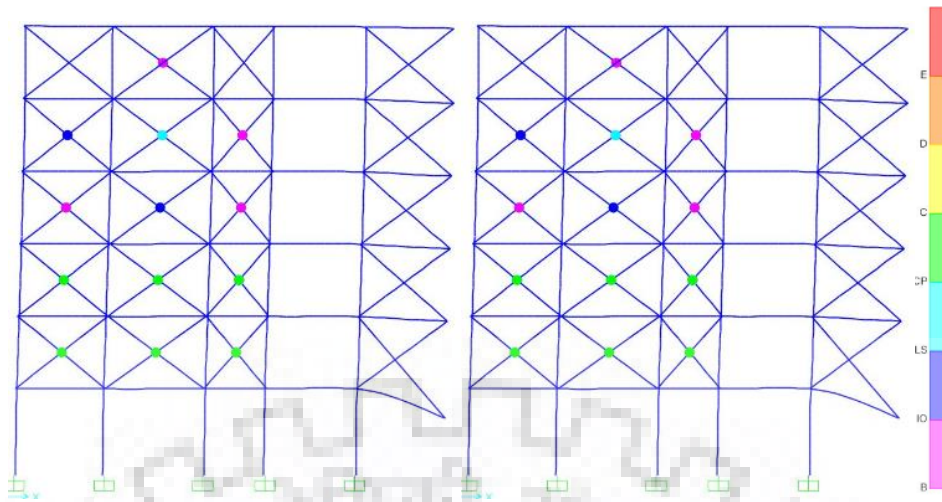


Figure 5.23 Hinge formation pattern for Case 3 in longitudinal direction in NLTH analysis

Figure 5.23 shows the hinge formation pattern in NLTH analysis, it can be seen that the hinges that were forming in the ground soft storey columns in the Case 1 are not forming now. The capacity has been increased by a significant amount.

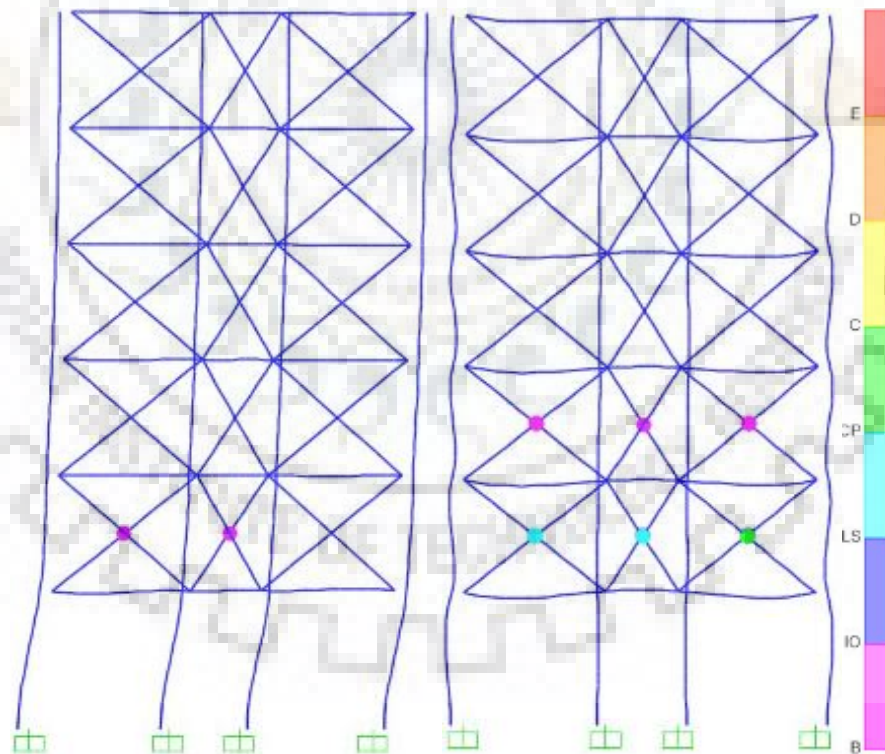


Figure 5.24 Hinge formation pattern for Case 3 in transverse direction condition in NLTH analysis

Similar behavior can also be seen in the transverse direction. Only the infill struts have formed hinges.

CHAPTER 6: CONCLUSIONS

In this study unreinforced masonry infill building with an open ground storey has been studied. The building was designed using response spectrum analysis without considering the effect of infills considering the fact that the infills are taken as nonstructural elements. After designing the infill was modelled and the behavior was assessed in nonlinear static and dynamic analysis. Two more cases were considered where the ground storey columns were designed for higher forces in an attempt to reduce the vulnerability of the ground storey columns. Performance were again studied for above mentioned analysis.

From the results it can be concluded that

1. There is a significant decrease in period due to the stiffening of the structure.
2. The seismic demand has increased and it can be explained in a way that stiffer the structure more forces it will attract.
3. Due to the open ground storey the stiffness variation between storeys is very high making the building vulnerable in soft storey mechanism.
4. From the Pushover analysis it can be concluded that the introduction of infills increases the strength but there is a reduction in ductility capacity.
5. Hinge formation pattern shows that hinges are forming in infills first and then propagates to beams and columns of ground storey.
6. Time history analysis the Inter-storey drift ratio and the hinge mechanism were studied and it can be seen that the drift ratio is very high at the first storey and the infill portion of building is having a much lesser drift ratio. Thus, it can be concluded that the portion is acting as one mass.
7. Hinge formation is following a same pattern as in pushover analysis.
8. After designing the ground storey columns for 2 times and 4 times the Case 1 design force the strength capacity has increased by 1.6 times.
9. The hinge formation pattern has also changed, the hinges are forming in infill struts of first storey and propagates to the upper storey struts.

REFERENCES

1. Agrawal, P. and Shrikhande, M. (2007). Earthquake Resistant Design of Structures. PHILearning Private Ltd., New Delhi, India.
2. ASCE 7-16 (2016). Minimum Design Loads and Associated Criteria for Buildings and Other Structures. Reston, Virginia.
3. ASCE/SEI 41 (2017). Seismic Evaluation and Retrofit of Existing Structures. Reston, Virginia.
4. Burton, S. E., Deierlein, F. (2014). "Simulation of Seismic Collapse in Nonductile Reinforced Concrete Frame Buildings with Masonry Infills. Journal of Structural Engineering." *American Society of Civil Engineers (ASCE)*, 140(8), A401-4016.
5. EN 1998-1/Eurocode 2 (2004). Design of structures for earthquake resistance – Part 1: General rules, seismic actions and rules for buildings. European Committee for Standardization, Rue de Stassart, Brussels
6. FEMA 356 (2000). Prestandard and Commentary for the Seismic Rehabilitation of Buildings. Federal Emergency Management Agency, Washington, DC.
7. Haldar, P., Singh, Y. (2012). "Modelling of URM infills and their effect on seismic behaviour of RC frame buildings." *The Open Constr Build Technol J* 6(Suppl. 1-M1), 35–41.
8. IS 875 (Part 1) (1987). Code of Practice for Design Loads (other than Earthquake) for Buildings and Structures - Dead Loads. *IS 875 (Part 1)*. Bureau of Indian Standards New Delhi, India.
9. IS 875 (Part 2) (1987). Code of Practice for Design Loads (other than Earthquake) for Buildings and Structures - Imposed Loads. Bureau of Indian Standards New Delhi, India.
10. IS 456 (2000). Plain and Reinforced Concrete – Code of Practice. Bureau of Indian Standards New Delhi, India.
11. IS 1893 (Part 1) (2016). Criteria of Earthquake Resistant Design of Structures: General Provisions and Buildings. Bureau of Indian Standards, New Delhi, India.
12. Kaushik, H. B., Rai, D. C., and Jain, S. K. (2007). "Stress-Strain Characteristics of Clay Brick Masonry under Uniaxial Compression." *Journal of Materials in Civil Engineering*, 19(9), 728-739.

13. *OriginPro 2017* [Computer software]. OriginLab Corporation, Northampton, MA.
14. PEER (Pacific Earthquake Engineering Research Centre). 2011. "PEER ground-motion database." (<https://ngawest2.berkeley.edu/site>).
15. SAP2000 *Ultimate version 20.0.0* [Computer software]. Computer and Structures, Inc., Berkeley, CA.

